# Phosphabenzenes as Monodentate π-Acceptor Ligands for Rhodium-Catalyzed Hydroformylation

**Bernhard Breit,*[a] Roland Winde,[a] Thomas Mackewitz,*[b] Rocco Paciello,[b] and Klaus Harms[c]**

*Dedicated to Professor Manfred Regitz on the occasion of his 65th birthday*

**Abstract:** A new class of phosphinine/rhodium catalysts for the hydroformylation of terminal and internal alkenes is presented in this study. A series of phosphabenzenes **1**–**14** has been prepared by condensation of phosphane or tris(trimethylsilyl)phosphane with the corresponding pyrylium salt. *Trans*-[(phosphabenzene)$_2$RhCl(CO)] complexes **21**–**25** have been prepared and studied spectroscopically and by X-ray crystal-structure analysis. The hydroformylation of oct-1-ene has been used to identify optimal catalyst preformation and reaction conditions. Hydroformylation studies with 15 monophosphabenzenes have been performed. The catalytic performance is dominated by steric influences, with the phosphabenzene **8**/rhodium system being the most active catalyst. Turnover frequencies of up to 45370 h$^{-1}$ for the hydroformylation of oct-1-ene have been determined. In further studies, hydroformylation activity toward more highly substituted alkenes was investigated and compared with the standard industrial triphenylphosphane/rhodium catalyst. The reactivity differences between the phosphabenzene and the triphenylphosphane catalyst increase on going to the more highly substituted alkenes. Even tetrasubstituted alkenes reacted with the phosphabenzene catalyst, whereas the triphenylphosphane system failed to give any product. In situ pressure NMR experiments have been performed to identify the resting state of the catalyst. A monophosphabenzene complex [(phosphinine **8**)Ir(CO)$_3$H] could be detected as the predominant catalyst resting state.

**Keywords:** homogeneous catalysis · hydroformylation · phosphabenzenes · phosphanes · rhodium

## Introduction

Hydroformylation of olefins is one of the most important homogeneously catalyzed industrial processes.[1] In the course of this reaction a new carbon–carbon bond is formed and, simultaneously, the synthetically valuable aldehyde function is introduced. If the chemo-, regio-, and stereoselectivity of such an appealing transformation could be controlled, new perspectives for both fine-chemical production and organic synthesis would arise. Major advances have been made toward this goal during the last decades.[2] Since the discovery of rhodium(I)–phosphine complexes as chemoselective hydroformylation catalysts,[3] carefully designed ligand modifications have led to improved catalysts.[2, 4] For example, Casey's concept of the natural bite angle stimulated the development of chelating diphosphine- and diphosphite-modified catalysts that allow the regioselective hydroformylation of terminal olefins in favor of the usually desired linear isomer.[5] Advances in the field of stereochemical control have been made by employing enforced substrate direction with the help of substrate-bound catalyst directing groups.[6] This concept has been applied to cyclic[7] and acyclic[8] olefinic building blocks. Additionally, chiral ligands such as BINAPHOS and others have been developed which allow for high asymmetric induction during the hydroformylation of certain prochiral alkenic substrates.[2, 9]

However, one of the long-standing and fundamental problems of hydroformylation chemistry—the low pressure hydroformylation of internal and more highly substituted olefins—still awaits a practical solution. Thus, it is known that the reactivity of hydroformylation catalysts decreases exponentially with the degree of olefin substitution.[10] Although rhodium–phosphine catalysts display a significantly higher reactivity toward the hydroformylation of terminal olefins compared with the cobalt–phosphine systems, their activity

[a] Prof. Dr. B. Breit, Dr. R. Winde
Organisch-Chemisches Institut
Ruprecht-Karls-Universität Heidelberg
Im Neuenheimer Feld 270, 69120 Heidelberg (Germany)
Fax: (+49) 6221-54-4205
E-mail: bernhard.breit@urz.uni-heidelberg.de

[b] Dr. T. Mackewitz, Dr. R. Paciello
BASF AG, Ammoniaklaboratorium, ZAG
67056 Ludwigshafen (Germany)

[c] Dr. K. Harms
Fachbereich Chemie der Philipps-Universität Marburg
Hans-Meerweinstrasse, 35043 Marburg (Germany)

  0947-6539/01/0714-3106 $ 17.50+.50/0 

toward hydroformylation of internal and higher 1,1-disubstituted olefins is still rather low.[10] In more detailed studies on the effect of modifying ligands with respect to the activity of the rhodium catalyst, some trends have been unraveled that may give a hint to a solution of this problem.[4a] Thus, strong and small σ-donor ligands may retard or even inhibit the reaction, while switching to stronger, π-acceptor ligands, such as phosphites, results in more active hydroformylation catalysts. In particular, the discovery of bulky phosphites as modifying ligands for rhodium catalysts has been an important advance in this field.[11] High catalyst activity for both hydroformylation of internal and terminal olefins has been observed. In situ NMR and IR spectroscopy has revealed that the enormous catalyst activity may be attributed to a monophosphite–rhodium complex as the catalytically active species.[12] Recently, similar phosphonite systems have been prepared with comparable ligand properties.[13] Unfortunately, a technical application of phosphites has been hampered by their inherent lability toward hydrolysis and a tendency to undergo degradation reactions.[14] Hence, the development of new classes of π-acceptor ligands remains an important task. In this context, we became interested in a hitherto unexplored class of potential π-acceptor ligands—the phosphabenzenes.[15] Although the first preparation of these systems by Märkl dates back to 1966,[15] no application as modifying ligands in homogenous catalysis was described until 1996.[16] Of particular interest is the electronic situation in phosphabenzenes compared with their nitrogen counterpart—the pyridine nucleus. Photoelectron spectroscopy[17] and ab initio calculations[18] show that the HOMO of a phosphabenzene has π-character with a large coefficient at the phosphorus atom. Note that the HOMO of pyridine is the lone pair at nitrogen. The LUMO of a phosphabenzene also has π-character with a large coefficient at the phosphorus atom. Its energy is lower than the corresponding pyridine LUMO. Hence, phosphabenzenes possess, at least qualitatively, an ideal frontier molecular-orbital situation for an efficient overlap with filled metal d-orbitals and, hence, the ability to act as π-acceptor ligands.

Here we wish to report in detail the preparation of phosphabenzenes and their coordination properties toward rhodium(I) centers, as well as their use as modifying ligands for the rhodium-catalyzed hydroformylation of terminal and internal olefins.[19]

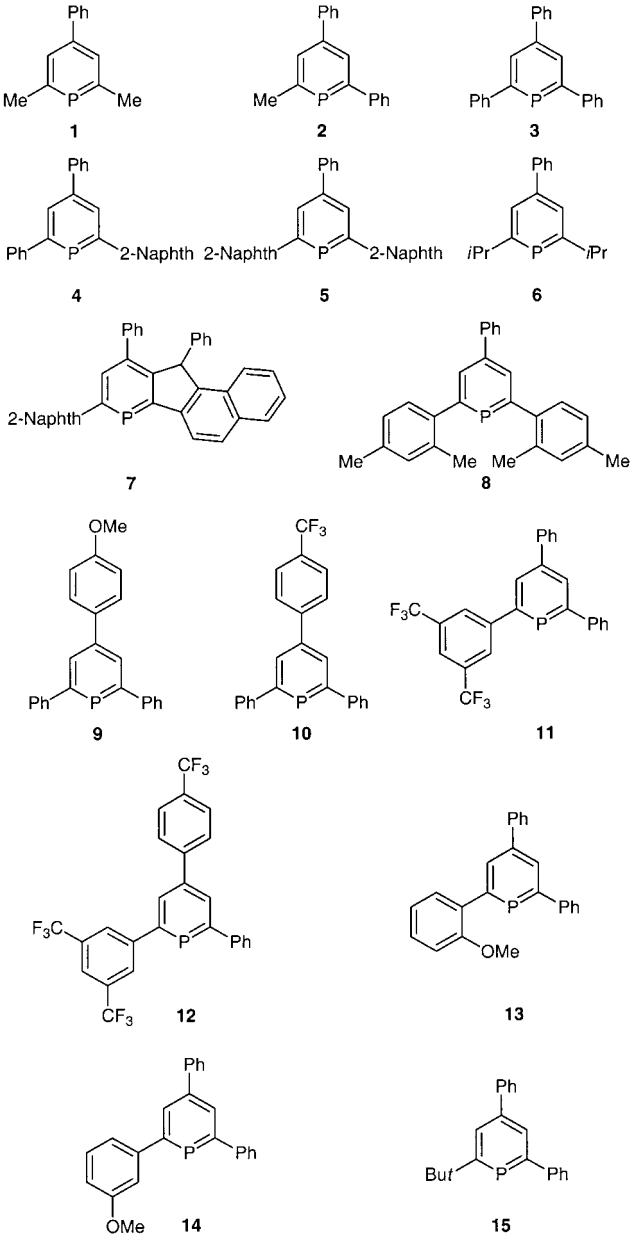


Scheme 1. Phosphabenzenes synthesized and investigated as ligands in rhodium-catalyzed hydroformylation.

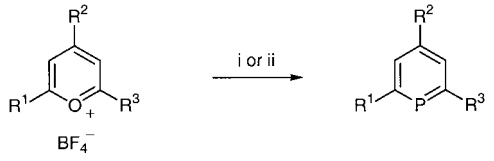


Scheme 2. i) 2–2.5 equiv $PTMS_3$, $CH_3CN$, reflux, 5 h (15–51%); ii) $PH_3$, 30 bar, *n*-butanol, 110 °C, 4 h (28–84%).

## Results

**Preparation of phosphabenzenes**: Phosphabenzene ligands **1**–**14** (Scheme 1) have been prepared employing a modified version of Märkl's original procedure.[20] Thus pyrylium tetrafluoroborates were treated in acetonitrile with excess tris(trimethylsilyl)phosphine at reflux temperature to give the phosphabenzenes **1**–**14** in moderate to fair yields, after chromatographic workup. Alternatively, pyrylium salts may be treated directly with phosphane gas (30 bar) at 110 °C to give the corresponding phosphabenzenes, usually in better yields (Scheme 2).[21]

The required pyrylium salts were obtained by tetrafluoroboric acid-mediated condensation of an appropriate chalcone derivative with a corresponding acetophenone system.[22] The chalcones were either prepared separately through aldol condensation of an arylmethylketone derivative with an aromatic aldehyde under basic conditions (catalytic amounts of activated barium hydroxide)[23] or generated in situ from

the same components in the presence of tetrafluoroboric acid[22] (see Experimental Section). 2,6-Dialkyl-substituted pyrylium salts were prepared according to published methods (Scheme 3).[24]

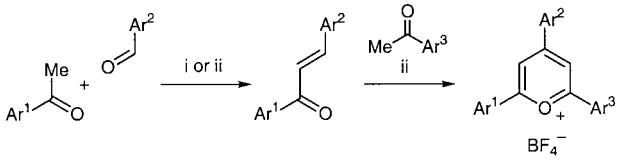

Scheme 3. i) 10 mol% $Ba(OH)_2$, ethanol, 20–80 °C; ii) $HBF_4$ (52% ethereal solution), 1,2-dichloroethane, reflux, 4 h (22–62%).

Pyrylium salt **16** was obtained in a one-pot operation upon treatment of chalcone **17** with tetrafluoroboric acid. Hence, the formation of **16** may be attributed to an interesting domino reaction sequence consisting of an intramolecular aromatic substitution to give **18** followed by condensation with enone **17** to furnish the polycyclic pyrylium tetrafluoroborate **16** (Scheme 4).

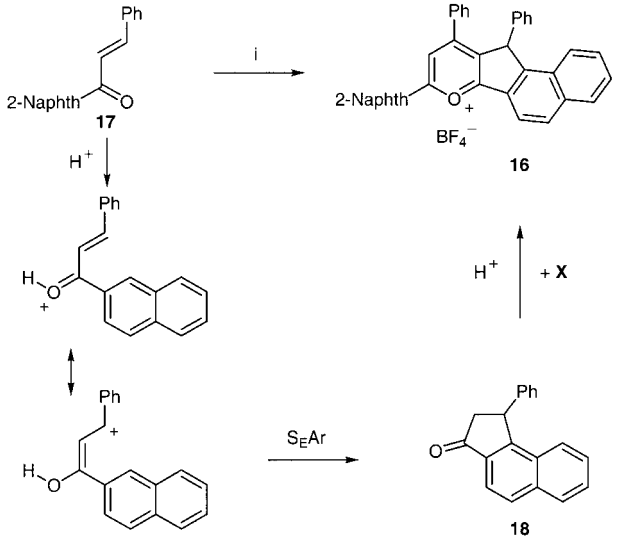

Scheme 4. i) $HBF_4$ (52% ethereal solution), 1,2-dichloroethane, reflux, 4 h (28%).

The *tert*-butyl substituted phosphabenzene **15** was obtained on treatment of $\alpha$-pyrone **19** with phosphaalkyne **20** in a cycloaddition-reversion sequence as introduced by Regitz et al. (Scheme 5).[25]

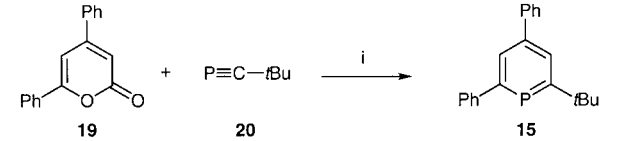

Scheme 5. i) Benzene, 140 °C, 3 d, Schlenk pressure vessel (54%).

**Rhodium complexes**: In order to study the ligand properties of phosphabenzenes in comparison with other known ligand classes, *trans*-[$L_2$RhCl(CO)] complexes were prepared. Thus, treating $[Rh(CO)_2Cl]_2$ with four equivalents of a corresponding phosphabenzene yielded the desired mononuclear *trans*-[($\eta^1$-phosphinine)$_2$RhCl(CO)] complexes **22**–**25** in quantitative yields (Scheme 6, Table 1).

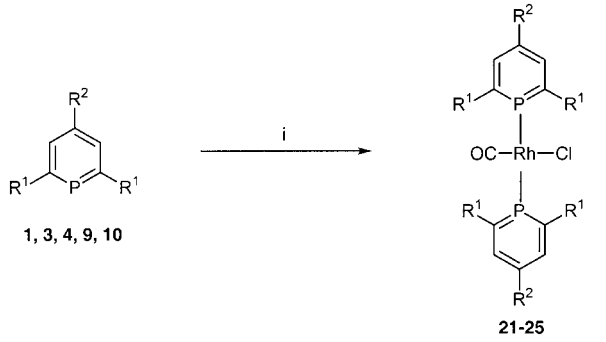

Scheme 6. Preparation of *trans*-[(phosphinine)$_2$RhCl(CO)] complexes **21**–**25**. i) $[Rh(CO)_2Cl]_2$, $CH_2Cl_2$, RT, 30 min, (quant.). **21**: $R^1$ = Me, $R^2$ = Ph, **22**: $R^1$ = Ph, $R^2$ = Ph, **23**: $R^1$ = 2-Naphth, $R^2$ = Ph, **24**: $R^1$ = Ph, $R^2$ = $C_6H_4$(*p*-OMe), **25**: $R^1$ = Ph, $R^2$ = $C_6H_4$(*p*-$CF_3$).

Table 1. *trans*-[(Phosphinine)$_2$RhCl(CO)] complexes **21**–**25** prepared according to Scheme 6.

| phosphinine | $R^1$ | $R^2$ | complex | $\tilde{\nu}$(CO) [$cm^{-1}$] |
|---|---|---|---|---|
| **1** | Me | Ph | **21** | 1998[26] |
| **3** | Ph | Ph | **22** | 1999 |
| **4** | 2-Naphth | Ph | **23** | 1998 |
| **9** | Ph | $C_6H_4$(*p*-OMe) | **24** | 2002 |
| **10** | Ph | $C_6H_4$(*p*-$CF_3$) | **25** | 2003 |

The $\eta^1$-coordination, as well as the symmetric nature of the complexes **22**–**25**, is reflected in their $^{31}$P NMR spectra. Thus, the phosphorus atoms absorb at $\delta$ = 166.1–173.8 as doublets with a $^1J$(P,Rh) coupling constant near the expected value of 175 Hz.[19b, 27] Compared with the free ligand, the $^{31}$P NMR signal is shifted about 20 ppm to higher field, which is typical for a $\eta^1$-coordinated phosphinine.[19b] The presence of the carbonyl ligand can be seen by $^{13}$C NMR spectroscopy. Thus, in a typical chemical-shift range of 180.7–181.9,[28] the carbonyl carbon resonates as a doublet of triplets with typical coupling constants of 65 Hz [$^1J$(C,Rh)] and 22 Hz [$^2J$(P,C)].[29] Additionally, the triplet splitting indicates the presence of two magnetically equivalent phosphabenzene nuclei. Final structural proof was obtained by an X-ray crystal-structure analysis of complex **22**. Its structure in the solid state is depicted in Figure 1.

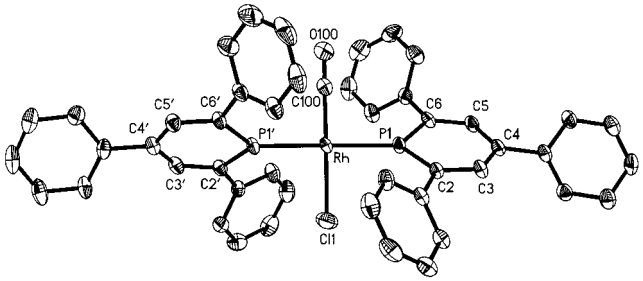


Figure 1. Ortep plot of the structure of *trans*-[(**3**)$_2$RhCl(CO)] (**22**) in the solid state.



0947-6539/01/0714-3108 $ 17.50+.50/0 *Chem. Eur. J.* **2001**, *7*, No. 14

The P–Rh lengths of 2.27 and 2.28 Å (Table 2) are noteworthy. They compare well with the analogous trispyrrol phosphine complex ($d$(Rh–P) = 2.28 Å)[30] as well as with the analogous bulky phosphite complex ($d$(Rh–P) = 2.29 Å, see Table 3),[31] but are significantly shorter than that found for the corresponding triphenylphosphine complex of 2.32 pm.[32] Since trispyrrolphosphine is known to be a strong π-acceptor ligand,[30] the similarity of the Rh–P bond lengths may reflect the back-bonding capability of the phosphabenzene nucleus. The least square planes of the phosphabenzene rings are tilted toward the Rh-P-CO-P-Cl least square plane by about 55.1° and 57.1°. Likewise, the *ortho*-phenyl substituents at the phosphabenzene nucleus are twisted out of the phosphabenzene plane by 40.2 – 53.2°.

The maximum angle that is formed from the van der Waals radii of L and rhodium is 172.5°. Note that this is not the classical cone angle as defined by Tolman,[33] since above and below the phosphabenzene plane the steric demand is much smaller. However, semiempirical calculations (PM3) allowed the rotation barrier about the P–Rh bond to be to estimated as less than 4 kcal mol$^{-1}$.[34] Thus, fast rotation of the phosphabenzene nuclei at the reaction temperatures employed is possible and, as a consequence, the steric demand of a phosphabenzene may be significantly larger than a fixed model would predict.

The IR stretching frequency of the CO ligand in *trans*-[$L_2$RhCl(CO)] is an ideal probe for determining the electronic properties of a phosphabenzene ligand. In analogy to the [LNi(CO)$_3$] complexes of Tolman,[33] a higher CO stretching frequency for a *trans*-[$L_2$RhCl(CO)] complex corresponds to a diminished electron density at the rhodium center and, hence, to a stronger back-bonding of the ligand, L.[35] Since, the rhodium complexes provide easy-to-interpret IR spectra with a single carbonyl band, these systems have found wide application as probes for the electronic properties of donor ligands.[35] The extensive literature available[36, 37] allows a rapid judgment of the electronic properties of a new ligand. Hence, for the phosphabenzene complex **22** the CO band was detected at 1999 cm$^{-1}$ which is about 21 cm$^{-1}$ higher in energy than that found for the corresponding triphenylphosphine complex,[30] but 14 cm$^{-1}$ lower in energy than that found in the complex with an tri(*ortho-tert*-butylphenyl)phosphite ligand[31] (see Table 1). This suggests that the electronic properties of phosphabenzenes are located in a range between phosphines and phosphites, with somewhat more similarity to the phosphite ligands.

IR spectra of the complexes were recorded in order to probe the electronic influence of substituents at the C2-, 4-, and 6-positions of the phosphabenzene nuclei on the stretching frequency of the CO ligand of the corresponding *trans*-[$L_2$RhCl(CO)] complexes (see Table 1). In all cases, only marginal changes in the CO IR band were observed. Thus, going from an *ortho/ortho′* dialkyl to an *ortho/ortho′* diaryl-substituted system did not have an effect. In addition, the exchange of phenyl substituents to more extended π-systems, such as the 2-naphthyl substituents, did not effect the CO stretching frequency. However, in the case of *para* substitution of the 4-aryl substituents, a shift to slightly larger wave numbers (1999 → 2003 cm$^{-1}$) was found. Interestingly, both a trifluoromethyl (**25**) and a methoxy substituent (**24**) caused a shift in the same direction. Hence, the methoxy group must exert its electronic influence, which is of course small, inductively through the σ-system. This would be in accordance with the observed out-of-plane geometry of all aryl substituents (see X-ray plot for complex **22** in Figure 1).

Table 2. Selected structural data for *trans*-[(**3**)$_2$RhCl(CO)] (**22**).

| | | | |
|---|---|---|---|
| Bond Lengths [Å] | | | |
| Rh–C(100) | 1.824(5) | C(4)–C(5) | 1.397(7) |
| Rh–P(1′) | 2.2724(12) | C(5)–C(6) | 1.397(6) |
| Rh–P(1) | 2.2805(12) | P(1′)–C(6′) | 1.715(5) |
| Rh–Cl(1) | 2.3465(14) | P(1′)–C(2′) | 1.722(5) |
| C(100)–O(100) | 1.104(7) | C(2′)–C(3′) | 1.390(6) |
| P(1)–C(2) | 1.716(4) | C(3′)–C(4′) | 1.392(7) |
| P(1)–C(6) | 1.723(5) | C(4′)–C(5′) | 1.396(7) |
| C(2)–C(3) | 1.381(6) | C(5′)–C(6′) | 1.394(6) |
| C(3)–C(4) | 1.414(6) | | |
| Bond Angles [°] | | | |
| C(100)-Rh-P(1′) | 89.27(16) | C(5)-C(4)-C(3) | 121.1(4) |
| C(100)-Rh-P(1) | 91.28(16) | C(6)-C(5)-C(4) | 125.0(4) |
| P(1′)-Rh-P(1) | 179.03(4) | C(5)-C(6)-P(1) | 121.2(4) |
| C(100)-Rh-Cl(1) | 178.65(18) | C(19)-C(6)-P(1) | 117.6(3) |
| P(1′)-Rh-Cl(1) | 90.08(5) | C(6′)-P(1′)-C(2′) | 105.8(2) |
| P(1)-Rh-Cl(1) | 89.39(5) | C(6′)-P(1′)-Rh | 124.39(16) |
| O(100)-C(100)-Rh | 179.7(5) | C(2′)-P(1′)-Rh | 129.78(16) |
| C(2)-P(1)-C(6 | 105.8(2) | C(3′)-C(2′)-P(1′) | 120.2(3) |
| C(2)-P(1)-Rh | 129.50(16) | C(7′)-C(2′)-P(1′) | 120.1(3) |
| C(6)-P(1)-Rh | 124.71(17) | C(2′)-C(3′)-C(4′) | 125.9(4) |
| C(3)-C(2)-P(1 | 120.7(3) | C(3′)-C(4′)-C(5′) | 122.0(4) |
| C(7)-C(2)-P(1) | 119.8(3) | C(6′)-C(5′)-C(4′) | 124.4(4) |
| C(2)-C(3)-C(4) | 126.1(4) | C(5′)-C(6′)-P(1′) | 121.5(4) |

Table 3. Comparison of the IR stretching frequency of CO and Rh–P bond lengths for selected *trans*-[$L_2$RhCl(CO)] complexes.

| Ligand | P(pyrrol)$_3$ | P[O(2-*t*-BuC$_6$H$_4$)]$_3$ | phosphinine **3** | PPh$_3$ |
|---|---|---|---|---|
| $\tilde{\nu}$ [cm$^{-1}$][a] | 2024[30] | 2013[31] | 1999[b] | 1978[30] |
| $d$(Rh–P) [Å] | 2.282(4)[30] | 2.2856(7)[31] | 2.2724(12)[b] | 2.323(6)[32] |

[a] in $CH_2Cl_2$; [b] this work.

**In situ high pressure NMR experiments**: For the rhodium triphenylphosphine system, it is known that under hydroformylation conditions, two phosphines are coordinated and an equilibrium between an equatorial – equatorial and an axial – equatorial species in a ratio of 85:15 exists.[38] For the bulky phosphite rhodium catalyst, in situ high pressure NMR and IR experiments indicate that a monophosphite rhodium complex is the prevalent species.[12] High pressure $^{31}$P and $^{1}$H NMR experiments were carried out in order to get information on the phosphabenzene rhodium system.

In an initial experiment, [Rh(COD)$_2$OTf] was dissolved in [D$_2$]dichloromethane, treated with two equivalents of the phosphabenzene ligand **8** and pressurized with 40 bars of syngas (CO/H$_2$ 1:1) for 3 h at 90 °C. After cooling to room temperature, the $^{31}$P NMR spectrum displayed a broad signal at $\delta = -154.5$, which split at $-90$ °C to a doublet with a typical $^{1}J$(P,Rh) coupling constant of 149 Hz. This result clearly shows that phosphabenzenes coordinate to rhodium under syngas pressure conditions. However, proton NMR spectroscopy revealed that the rhodium species belonging to this $^{31}$P NMR resonance is not the trigonal-bipyramidal hydride complex

typically seen in hydroformylation catalysis (no hydride signal could be detected).

In order to characterize this hydride complex and to clarify the number of ligands attached to the metal center in such a species, we switched to the more stable iridium complexes. Hence, $[Ir(CO)_2acac]$ (acac = acetylacetonate) and two equivalents of phosphabenzene **8** were dissolved in $[D_2]$dichloromethane in a high pressure NMR tube and treated at 90 °C with 40 bar syngas pressure. NMR spectra were recorded at −90 °C. In addition to the free phosphabenzene ligand (ca. 50 %), the phosphorus NMR spectra show two phosphorus signals at $\delta = 143.9$ and 144.3. The proton NMR spectrum shows a metal hydride signal at $\delta = -11.83$ as a doublet with a $^2J(H,P)$ coupling of 23.2 Hz. This doublet collapses to a singlet in the $^{31}P$-decoupled $^1H$ NMR experiment. Interestingly, $^1H\{^{31}P\}$ COSY spectra showed one cross peak for both $^{31}P$ signals at $\delta = 143$ with the metal hydride signal at $\delta = -11.83$.

These data are consistent with the presence of an $\eta^1$-monophosphabenzene hydrido-iridium complex. The $^{31}P$ NMR spectrum suggests that this species presumably exists as two resolved rotamers at −90 °C. The splitting of the hydride signal to a doublet, as well as the presence and quantity of free phosphabenzene ligand, is consistent with the coordination of only one phosphabenzene to the metal center under syngas pressure. The small size of the $^2J(H,P)$ coupling constant suggests an equatorial position for the phosphabenzene nucleus.[39] Hence, iridium complex **26** is the predominant species and, thus, may also represent the resting state of the corresponding rhodium catalyst (Figure 2).

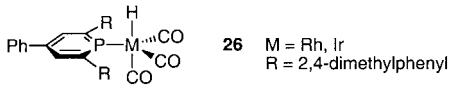


**26** M = Rh, Ir
R = 2,4-dimethylphenyl

Figure 2. Proposed (Rh) and experimentally observed (Ir) mono-phosphabenzene tris-carbonyl $d^9$-metal complexes **26** under 40 bar syngas pressure.

The coordination behavior of phosphabenzenes mirrors that of the bulky phosphite ligands.[12] Hence, one might expect a related catalytic activity for the phosphabenzene class of ligands.

**Hydroformylation experiments: oct-1-ene**: In order to evaluate the phosphabenzene rhodium system as a catalyst for the hydroformylation reaction, oct-1-ene was chosen as a first test substrate. The possible reaction pathways and reaction products under hydroformylation conditions are depicted in Scheme 7. Thus, in a single hydroformylation experiment, one can learn about the regioselectivity of the hydroformylation of the terminal alkene and the potential for isomerizing terminal to internal alkenes, as well as the ability to hydroformylate internal alkenes.

At the beginning of a kinetic experiment, one has to ensure that all of the rhodium precursor has been transferred into the active hydroformylation catalyst; otherwise the observed kinetic data would reflect the activation phase for the catalyst. Hence, we began with an investigation to identify the ideal

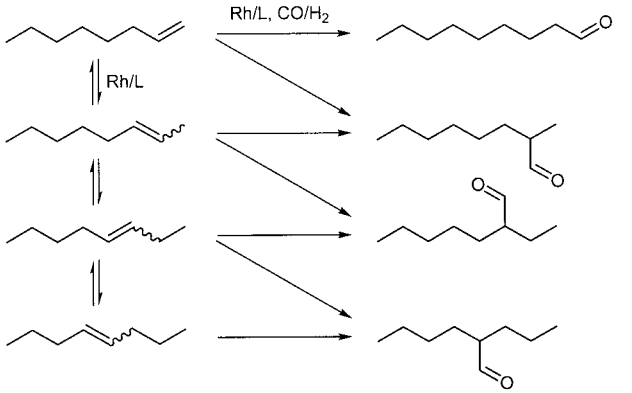


Scheme 7. Possible reaction pathways and products in the course of a hydroformylation reaction with oct-1-ene or oct-2-ene.

preformation conditions for the rhodium/phosphabenzene catalyst system. 2,4,6-Triphenylphosphabenzene (**3**) was chosen as the standard ligand. Pretreatment of a mixture of $[Rh(CO)_2acac]$ and 20 equiv. of phosphabenzene **3** in toluene for 30 min at 75 °C with 10 bar $CO/H_2$, followed by addition of oct-1-ene through a pressure vessel gave the kinetic data depicted in Figure 3b.

When compared with the control experiment in the absence of phosphabenzene ligand (see Figure 3a), it becomes clear that deactivation of the rhodium had occurred. This may be attributed to the formation of unreactive rhodium clusters; a phenomenon which has been observed previously.[40] In the second experiment, see Figure 3c, phosphabenzene **3** was allowed to react with $[Rh(CO)_2acac]$ in toluene for 45 min at RT to ensure coordination to the rhodium center. After addition of oct-1-ene and transfer to an autoclave, the reaction mixture was heated to 75 °C and subsequently pressurized with 10 bar $H_2/CO$ (1:1). The kinetic data obtained clearly show that this procedure provided an active hydroformylation catalyst. Interestingly, a strong tendency toward isomerization was observed. One might speculate that not all of the rhodium precursor was transferred into the active rhodium phosphabenzene catalyst at the beginning of the kinetic experiment. However, it was assumed that at the end of a complete hydroformylation experiment all of the rhodium(I) precursor should exist as an active hydroformylation catalyst. Hence, we let the catalyst do a complete hydroformylation run of oct-1-ene for 15 h. After this time, GC analysis showed complete consumption of the starting material. The product mixture consisted exclusively of C9 aldehydes. More importantly, $^{31}P$ NMR analysis of the mixture showed that no phosphabenzene degradation had occurred during that first hydroformylation run; this indicated the stability of phosphabenzene ligands under hydroformylation conditions.[41] Next, a new hydroformylation run could be started cleanly by addition of a second portion of oct-1-ene. GC analysis provided the kinetic data depicted in Figure 3d, which show clean hydroformylation catalysis. Hence, this preformation procedure became our standard and was subsequently applied to all further hydroformylation experiments with oct-1-ene.

For all subsequently reported hydroformylation experiments, a complete set of kinetic data was recorded. In all



0947-6539/01/0714-3110 $ 17.50+.50/0 *Chem. Eur. J.* **2001**, *7*, No. 14

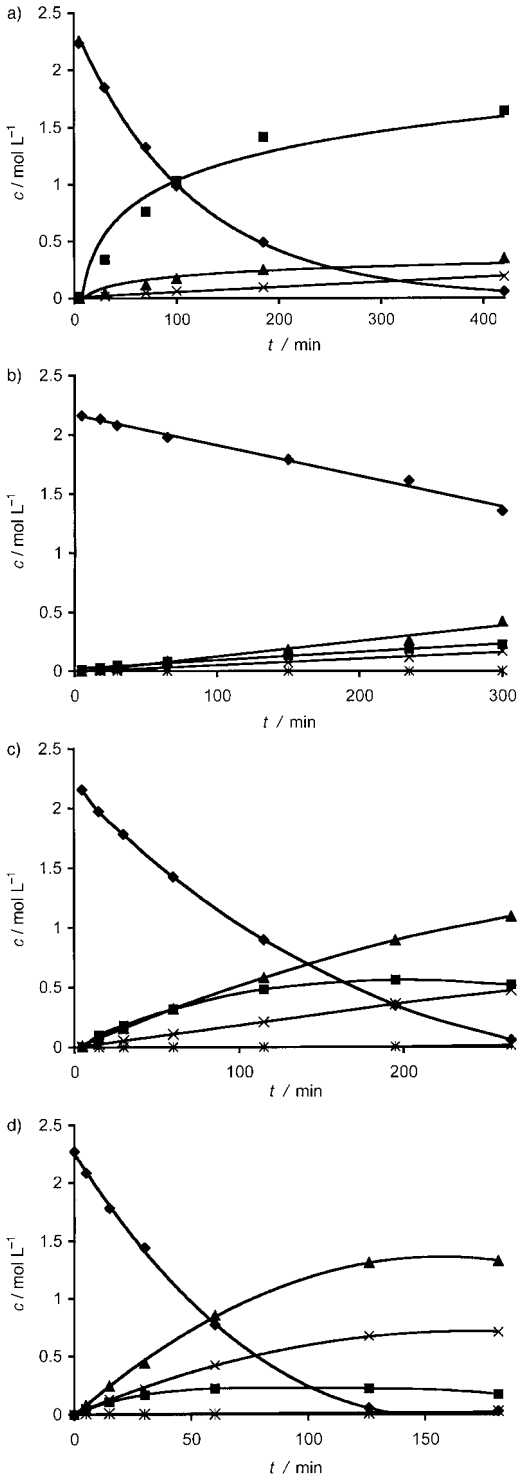


Figure 3. Kinetics of hydroformylation experiments of oct-1-ene a) with $[Rh(CO)_2acac]$ and b–d) with $[Rh(CO)_2acac]$/**3** after different catalyst preformation procedures; ◆ = oct-1-ene, ■ = internal octene isomers, ▲ = *n*-nonanal, × = 2-methyloctanal, * = 2-ethylheptanal. Initial oct-1-ene concentration ($c_0 = 2.27$ M) in toluene; for a) oct-1-ene/Rh = 4166:1, for b–c) oct-1-ene/phosphinine **3**/Rh = 4166:20:1. a) Control experiment without phosphabenzene ligand; $[Rh(CO)_2acac]$ at 75 °C, 10 bar ($H_2$/CO 1:1), toluene ($c_0 = 2.27$ M). b) $[Rh(CO)_2acac]$/**3** in toluene were allowed to react for 30 min at 75 °C, 10 bar ($H_2$/CO 1:1) followed by addition of oct-1-ene through a pressure chamber. c) $[Rh(CO)_2acac]$/**3** in toluene were allowed to react for 30 min at RT followed by addition of oct-1-ene. The mixture was transferred to a preheated autoclave (75 °C) and the reaction started by addition of 10 bar $H_2$/CO (1:1). d) Second run experiment: 90 °C, 10 bar $H_2$/CO (1:1). For details see Experimental Section.

experiments, complete consumption of octenes was reached after a reaction period of about 4 h.

As shown in Figure 3d, the hydroformylation reaction with oct-1-ene is zeroth order under our conditions, at least up to a conversion of 30 %. That is, turn over frequencies in this range are independent of conversion. This allows comparison of the catalytic activity by determining the turnover frequencies (TOF) within the low conversion range (see Tables 4–8, below). Importantly, at low conversions, the internal olefins formed by isomerization of the terminal olefin have not yet been attacked. Hence, determination of turnover frequencies for olefin isomerization is possible as well.

**Influence of the ligand/rhodium ratio**: The phosphabenzene **3**/rhodium ratio necessary to ensure that all the rhodium centers are converted in situ into the active complexes and that all the effects observed could be ascribed to the varied parameters was determined. Ligand/rhodium ratios of 2:1, 20:1 and 91:1 were explored. At low phosphabenzene concentrations (Table 4, entry 1), low hydroformylation but significant isomerization activity was observed. This indicates that not all rhodium species have been transferred into catalytically active phosphabenzene/rhodium complexes. Similar effects are known for bulky phosphite/rhodium systems.[42] Increasing the ligand concentration (20 equiv, Table 4, entry 2) provided a catalyst system with high hydroformylation activity and a lower tendency for isomerization. The ratio of $TOF_{ald}/TOF_{iso}$ increased to 4.6:1; this resulted in a maximum value of 9.8 % for internal alkene formation. Increasing the ligand concentration further (91 equiv, Table 4, entry 3) slightly decreased the hydroformylation rate, but almost suppressed isomerization activity. These results indicate that a ligand/Rh ratio of 20:1 is sufficient to transfer all of the rhodium into catalytically active species. Even though at higher L/Rh ratios the isomerization rate could be decreased further, the lower ligand loading (20:1) was chosen as the standard for all further experiments.

Table 4. Influence of ligand/rhodium ratio on the hydroformylation of oct-1-ene with $[Rh(CO)_2acac]$/**3**, at 90 °C, 10 bar ($CO/H_2$, 1:1) in toluene ($c_0 = 2.27$ M) (oct-1-ene/Rh, 4166:1).[a]

| | L/Rh | Conv. [%] | $TOF_{ald}$ [$h^{-1}$] | $TOF_{iso}$ [$h^{-1}$] | $TOF_{ald}/TOF_{iso}$ | $Iso^{max}$ [%] | $n/iso^{max}$ |
|---|---|---|---|---|---|---|---|
| 1 | 2 | 19.4 | 955 | 721 | 1.3 | 26.5 | 2.7 |
| 2 | 20 | 21.6 | 2801 | 610 | 4.6 | 9.8 | 2.0 |
| 3 | 91 | 14.6 | 2442 | 54 | 45.2 | 2.7 | 1.9 |

[a] $TOF_{ald}$ = turnover frequency of aldehyde formation; $TOF_{iso}$ = turnover frequency of alkene isomerization.

**Influence of reaction temperature**: An increase of the reaction temperature from 70 °C to 90 °C increased the rates of both hydroformylation and isomerization. However, on going further to 110 °C, a dramatic drop for the rate of hydroformylation was observed. Conversely, the isomerization rate largely increased. Hence, 90 °C became the reaction temperature of choice, since a good compromise between rapid hydroformylation and modest isomerization could be achieved (Table 5).

Table 5. Influence of temperature on the hydroformylation of oct-1-ene with [Rh(CO)$_2$acac]/**3**, at 10 bar (CO/H$_2$ 1:1) in toluene ($c_0 = 2.27$ M) (oct-1-ene/**3**/Rh, 4166:20:1).

| | $T$ [°C] | Conv. [%] | TOF$_{ald}$ [h$^{-1}$] | TOF$_{iso}$ [h$^{-1}$] | TOF$_{ald}$/TOF$_{iso}$ | Iso$^{max}$ [%] | $n$/iso$^{max}$ |
|---|---|---|---|---|---|---|---|
| 1 | 70 | 19.6 | 1557 | 48 | 32.4 | 3.9 | 2.2 |
| 2 | 90 | 21.6 | 2801 | 610 | 4.6 | 9.8 | 2.0 |
| 3 | 110 | 27.1 | 1075 | 3316 | 0.3 | 53.0 | 3.3 |

**Influence of reaction pressure**: To study the influence of the syngas pressure, experiments at 5, 10, 20 and 40 bars were performed (see Table 6). A strong increase of hydroformylation and isomerization rate was observed. While the hydroformylation rate showed an almost fivefold increase, the isomerization rate increased only by a factor of three on going from five to 40 bar total pressure (CO/H$_2$ 1:1). This behavior differs from that of the bulky phosphite/rhodium catalysts, which show only a marginal rate increase at higher syngas pressures.[42] The lowest isomerization was found at 10 bar with a maximum amount of 9.8 % for the formation of internal alkenes. Hence, 10 bar syngas pressure was selected as the optimal reaction pressure for all further studies.

Table 6. Influence of syngas pressure (CO/H$_2$, 1:1) on the hydroformylation of oct-1-ene with [Rh(CO)$_2$acac]/**3**, at 90 °C in toluene ($c_0 = 2.27$ M) (oct-1-ene/**3**/Rh, 4166:20:1).

| | p [bar] | Conv. (%) | TOF$_{ald}$ [h$^{-1}$] | TOF$_{iso}$ [h$^{-1}$] | TOF$_{ald}$/TOF$_{iso}$ | Iso$^{max}$ (%) | $n$/iso$^{max}$ |
|---|---|---|---|---|---|---|---|
| 1 | 5 | 41.1 | 1111 | 550 | 2.0 | 13.2 | 1.9 |
| 2 | 10 | 36.5 | 2437 | 610 | 4.0 | 9.8 | 2.0 |
| 3 | 20 | 31.6 | 4371 | 883 | 4.9 | 23.5 | 2.4 |
| 4 | 40 | 40.1 | 5141 | 1550 | 3.3 | 14.1 | 2.1 |

**Influence of ligand structure**: In order to determine how steric effects at the phosphabenzene ligands influence the hydroformylation reaction, a series of monophosphabenzene ligands was tested under standardized conditions (see Table 7). The results depicted in the table show that increasing the steric demand of the *ortho*/*ortho*′-substituents at the phosphabenzene leads to more active catalysts. Going from dimethyl derivative **1** (Table 7, entry 1) to ligand **8** (Table 7, entry 8) led to a fivefold increase of the hydroformylation rate. Likewise isomerization toward internal alkenes increased from 1.3 % for ligand **1** up to a maximum of 20.3 % for **8**. However, ligand **15** with a *tert*-butyl/phenyl substitution pattern in *ortho*/*ortho*′-position did not provide an active hydroformylation catalyst.

Table 7. Influence of ligand structure (sterics) on the hydroformylation of oct-1-ene with [Rh(CO)$_2$acac]/L, at 90 °C, 10 bar (CO/H$_2$ 1:1) in toluene ($c_0 = 2.27$ M) (oct-1-ene/L/Rh 4166:20:1).

| | Ligand | Conv. [%] | TOF$_{ald}$ [h$^{-1}$] | TOF$_{iso}$ [h$^{-1}$] | TOF$_{ald}$/TOF$_{iso}$ | Iso$^{max}$ [%] | $n$/iso$^{max}$ |
|---|---|---|---|---|---|---|---|
| 1 | **1** | 28.2 | 1111 | 18 | 61.7 | 1.3 | 1.8 |
| 2 | **2** | 24.6 | 1711 | 451 | 3.8 | 18.0 | 2.4 |
| 3 | **3** | 21.6 | 2801 | 779 | 3.6 | 9.8 | 2.0 |
| 4 | **4** | 35.0 | 2866 | 121 | 23.7 | 3.0 | 1.9 |
| 5 | **5** | 31.4 | 1975 | 94 | 21.1 | 3.7 | 2.0 |
| 6 | **7** | 32.5 | 2522 | 242 | 10.4 | 5.2 | 1.5 |
| 7 | **6** | 33.5 | 3612 | 1964 | 1.8 | 15.3 | 2.2 |
| 8 | **8** | 11.5 | 5751 | 2071 | 2.8 | 20.3 | 3.3 |

In order to probe whether an electronic modification of the phosphabenzene nucleus would have any effect on the catalytic properties of the resulting rhodium/phosphabenzene catalyst, ligands **9**–**12** were tested.

Experiments with ligands **3**, **10** and **11** (Table 8, entries 1–3) show only a marginal influence of the CF$_3$ or MeO group in the *para*-position to the 4-aryl substituent at the phosphabenzene nucleus. This is consistent with the small change in the CO stretching frequency found for the rhodium complexes **22**, **24**, and **25**, which indicates only minor electronic effects on the rhodium center. Introducing two CF$_3$ groups in the 3- and 5-positions of an *ortho*-aryl substituent (ligand **11**, Table 8, entry 4) lowered the catalytic activity. However, adding one further CF$_3$ group at the 4-position of the *para* aryl group (ligand **12**, Table 8, entry 5) leads to a more active hydroformylation catalyst.

Table 8. Influence of ligand structure (electronics) on the hydroformylation of oct-1-ene with [Rh(CO)$_2$acac]/L, at 90 °C, 10 bar (CO/H$_2$ 1:1) in toluene ($c_0 = 2.27$ M) (oct-1-ene/L/Rh 4166:20:1).

| | Ligand | Conv. [%] | TOF$_{ald}$ [h$^{-1}$] | TOF$_{iso}$ [h$^{-1}$] | TOF$_{ald}$/TOF$_{iso}$ | Iso$^{max}$ [%] | $n$/iso$^{max}$ |
|---|---|---|---|---|---|---|---|
| 1 | **3** | 21.6 | 2801 | 779 | 3.6 | 9.8 | 2.0 |
| 2 | **9** | 30.6 | 2443 | 110 | 22.2 | 3.2 | 1.8 |
| 3 | **10** | 21.8 | 2655 | 863 | 3.1 | 12.6 | 2.0 |
| 4 | **11** | 27.1 | 1951 | 200 | 9.8 | 4.6 | 2.0 |
| 5 | **12** | 32.8 | 4583 | 801 | 5.7 | 10.7 | 1.9 |
| 6 | **13** | 27.8 | 2181 | 180 | 12.1 | 5.5 | 1.9 |
| 7 | **14** | 26.4 | 1995 | 175 | 11.4 | 5.5 | 1.9 |

In a further attempt, we explored whether the introduction of a weakly coordinating donor into the phosphabenzene system might influence the isomerization propensity. One may assume that such an additional hemilabile coordinative function might suppress the formation of coordinatively unsaturated rhodium intermediates, and thus reduce olefin isomerization. Hence, methoxy substituted ligands **13** and **14** were tested (Table 8, entries 6 and 7). Compared with the standard triphenylphosphabenzene ligand **3** system, the hydroformylation activity for both the 2- and 3-methoxy derivatives is only slightly diminished. However, isomerization is significantly reduced. In both cases a maximum of 5.5 % internal olefin formation was detected.

The above experiments identified the rhodium catalyst obtained from phosphabenzene **8** as the most active for hydroformylation of oct-1-ene. Figure 4 shows the concentration of starting material and products as a function of time under a) standard conditions (90 °C, 10 bar syngas) and b) enforced reaction conditions (130 °C, 40 bar syngas). Interestingly, for the standard conditions, a conversion of oct-1-ene of 78 % was reached after 30 min. In addition to aldehydes a maximum of 20.3 % internal octenes had formed at this point of time. After 30 minutes, a decrease in the concentration of internal olefins was accompanied by an increase in 2-ethyl-



0947-6539/01/0714-3112 $ 17.50+.50/0 *Chem. Eur. J.* **2001**, *7*, No. 14

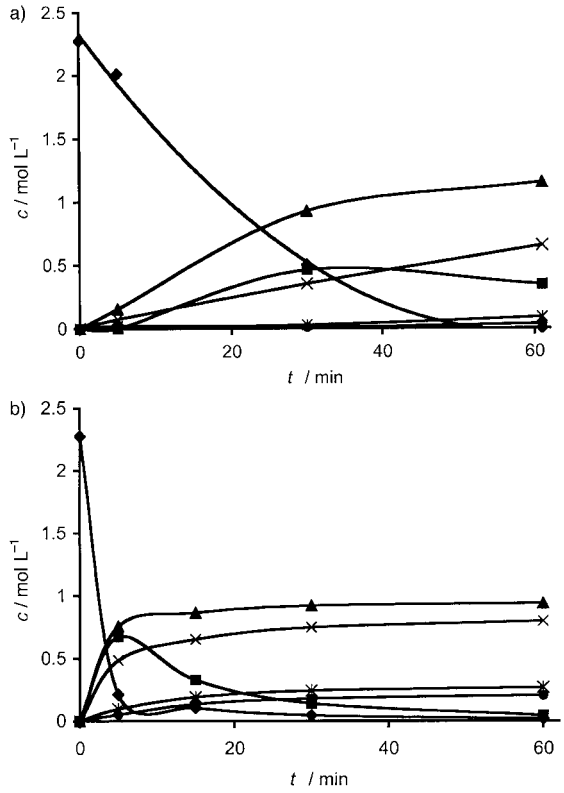


Figure 4. Kinetics of the hydroformylation of oct-1-ene with [$Rh(CO)_2$-acac]/**8**, in toluene ($c_0 = 2.27$ M) (oct-1-ene/**8**/Rh, 4166:20:1) at a) 90 °C, 10 bar ($CO/H_2$ 1:1) and b) 130 °C, 40 bar ($CO/H_2$ 1:1); ◆ = oct-1-ene, ■ = internal octene isomers, ▲ = *n*-nonanal, × = 2-methyl octanal, * = 2-ethylheptanal.

heptanal and 2-propylhexanal concentration. Hence, internal olefins were attacked and hydroformylated; this indicated that phosphabenzene/rhodium catalysts should be suited to hydroformylate internal and more highly substituted olefins.

Increasing the reaction temperature to 130 °C and the syngas pressure to 40 bar provided an extremely active hydroformylation catalyst (Figure 4b). Here, a maximum turnover frequency of 45370 h$^{-1}$ was observed for aldehyde formation. Complete consumption of starting material was reached after only 30 min. Additionally, complete consumption of the internal octenes formed by prior alkene isomerization was observed after 60 min.

Since phosphabenzene **8** evidently provided the most active rhodium catalyst for the hydroformylation of oct-1-ene, it was decided to employ this system in all subsequent studies on hydroformylation of higher-substituted alkenes.

### Hydroformylation of more highly substituted olefins

*Cyclohexene*: Cyclohexene was selected in order to determine the potential of phosphabenzene rhodium catalysts for hydroformylation of internal olefins, since it allows observation of hydroformylation formally undisturbed by olefin isomerization.

Hydroformylation was performed at 90 °C and 40 bar syngas pressure. For the phosphabenzene rhodium system, an initial turnover frequency of 1959 h$^{-1}$ was detected (see Scheme 8, Figure 5). The standard triphenylphosphane/rhodium system was about 18 times slower with an initial TOF of 109 h$^{-1}$.

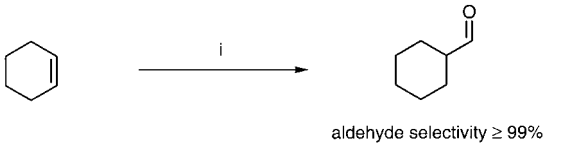


Scheme 8. Hydroformylation of cyclohexene. i) Rh/L, $CO/H_2$, 40 bar, $T$ = 90 °C, toluene. TOF [h$^{-1}$] L = $PPh_3$: 109, L = **8**: 1959.

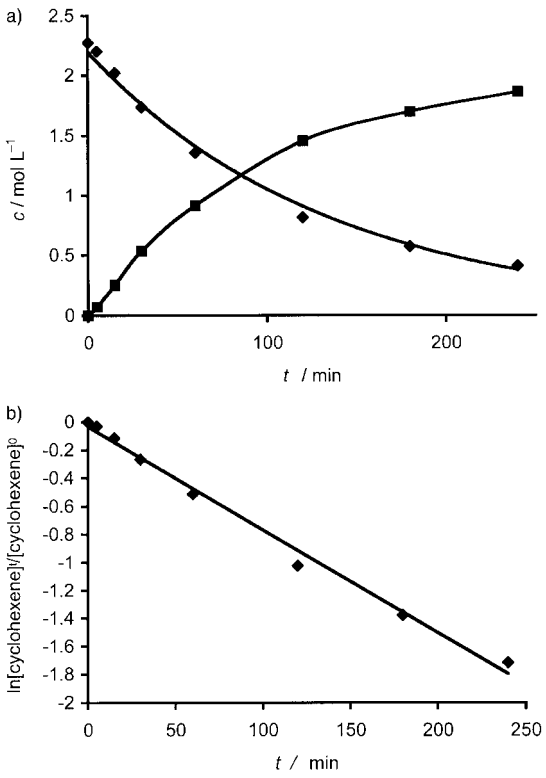


Figure 5. a) Kinetics of the hydroformylation of cyclohexene with phosphinine **8**/[$Rh(CO)_2$acac] at 90 °C, 40 bar in toluene ($c_0 = 2.63$ M) for 4 h (cyclohexene/L/Rh, 4166:20:1), ▲ *c*(cyclohexene), ■ *c*(cyclohexane carbaldehyde); b) Logarithmic plot of cyclohexene concentration against time ($k_{hydroform.} = 7.3 \times 10^{-3}$ s$^{-1}$).

Surprisingly, the TOF for hydroformylation of cyclohexene with the phosphine/rhodium catalyst is only moderately lower than the TOF upon hydroformylation of oct-1-ene. This is rather different behavior from the bulky monodentate phosphites. Their catalytic activity drops by about a factor of 80 on going from oct-1-ene to cyclohexene as the substrate. Interestingly, the reaction is first order with respect to substrate (Figure 5b); this indicates that olefin coordination has become the rate determining step.

*Oct-2-ene*: A more complex situation is given for oct-2-ene as an internal olefin substrate. In addition to hydroformylation of the internal olefin, it is also of interest to see whether olefin isomerization occurs simultaneously. An *n*-selective isomerizing hydroformylation might give rise to the formation of linear aldehydes. Formation of oct-1-ene and subsequent hydroformylation, for example, could then provide *n*-nonanal. Such an isomerizing hydroformylation could be of industrial

Table 9. Results of the hydroformylation of oct-2-ene (*cis/trans*, 77:23) with [Rh(CO)$_2$acac]/**8** and TPP at 90 °C, 10 bar (CO/H$_2$ 1:1) in toluene ($c_0$ = 7.13 M) after 4 h (oct-2-ene/L/Rh, 7222:20:1).

| Ligand | oct-2-ene [mol %] | oct-3/4-ene [mol %] | nonanal [mol %] | 2-methyloctanal [mol %] | 2-ethylheptanal [mol %] | 2-propylhexanal [mol %] |
|---|---|---|---|---|---|---|
| **8** | 0 | 1 | 24 | 43 | 18 | 14 |
| $PPh_3$ | 31 | 5 | 3 | 42 | 17 | 2 |

significance with respect to "raffinate 2", a product of the steam cracking process, which is a mixture of butenes.[4b]

The complete set of potential reaction pathways for an isomerizing hydroformylation of oct-2-ene is depicted in Scheme 7. The experiment was carried out at 90 °C and 10 bar syngas pressure. After 4 h, the phosphabenzene catalyst had transferred all the starting material into aldehyde products (see Table 9). Interestingly, 24 % of *n*-nonanal was formed. The initial TOF for aldehyde formation was 6933 h$^{-1}$. If one assumes an intrinsic linearity for the rhodium/**8** catalyst of 72 %, as observed in the course of hydroformylation of oct-1-ene (see above), one can conclude that 33 % of the oct-2-ene was isomerized to oct-1-ene (or its corresponding rhodium complex) prior to hydroformylation. For the triphenylphosphine catalyst, 36 % of octenes are left unconsumed after 4 h. Additionally, only 5 % of nonanal could be detected. Thus, the phosphabenzene/rhodium catalyst is substantially more active toward hydroformylation of internal olefins and, additionally, shows a significant tendency for producing terminal aldehydes from internal olefins.

*1,1-Disubstituted alkenes*: Isobutene was selected as a representative example for the class of 1,1-disubstituted alkenes (Scheme 9). Identical hydroformylation experiments with the

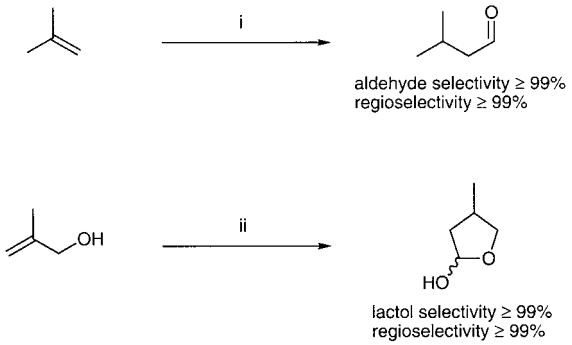


Scheme 9. Hydroformylation of 1,1-disubstituted alkenes. i) Rh/L, CO/H$_2$, 30 bar, $T$ = 80 °C, toluene. TOF [h$^{-1}$] L = $PPh_3$: 332, L = **8**: 3132. ii) Rh/L, CO/H$_2$, 20 bar, $T$ = 90 °C, toluene. TOF [h$^{-1}$] L = $PPh_3$: 1317, L = **8**: 3291.

rhodium/phosphabenzene **8** and the standard rhodium/triphenylphosphine catalyst were performed. The reaction mixture was analyzed after a reaction period of 4 h. Once again, the phosphabenzene/rhodium catalyst was about 100 times faster than the standard rhodium/triphenylphosphine system. The aldehyde selectivity and regioselectivity were in both cases greater than 99 %.

Methallyl alcohol was chosen to study a functionalized 1,1-disubstituted alkene (Scheme 9). Hydroformylation with both the standard rhodium/triphenylphosphine catalyst as well as with the phosphabenzene/rhodium system proceeded smoothly to furnish the corresponding lactol as a mixture of anomers in greater than 99 % selectivity. Notably, the phosphabenzene/rhodium system was about 2.5 times faster.

**Tri- and tetrasubstituted alkenes**: Trisubstituted alkenes such as $\alpha$-pinene are among the least reactive alkenes with respect to the hydroformylation reaction. While the triphenylphosphine/rhodium system failed to provide any aldehyde product under the reaction conditions employed, the rhodium/phosphabenzene catalyst transformed $\alpha$-pinene smoothly into the corresponding aldehyde (Scheme 10). Aldehyde selectivity was greater than 99 % and combined with good regio- as well as diastereoselectivity.

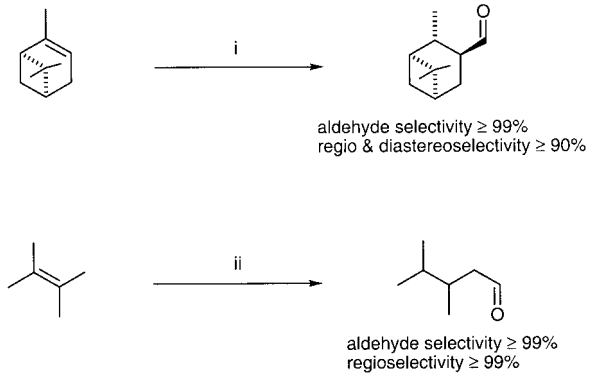


Scheme 10. Hydroformylation of tri- and tetrasubstituted alkenes. i) Rh/**8**, CO/H$_2$, 60 bar, $T$ = 80 °C, toluene. TOF = 56 h$^{-1}$. ii) Rh/L, CO/H$_2$, 60 bar, $T$ = 100 °C, toluene. TOF [h$^{-1}$] L = $PPh_3$: < 1, L = **8**: 118.

The hydroformylation of tetrasubstituted alkenes, such as tetramethylethylene, is more difficult.[10] Hydroformylation may be achieved under very high pressures and temperatures with an unmodified cobalt catalyst.[43] However, to the best of our knowledge, no efficient hydroformylations in the low to medium pressure range with ligand-modified rhodium catalysts are known. Interestingly, the rhodium/phosphabenzene **8** catalyst is even able to consume tetramethylethylene as a substrate for hydroformylation under the rather mild reaction conditions of 100 °C and 60 bar syngas pressure (Scheme 10). The exclusive reaction product was 3,4-dimethylpentanal, which arises through successive alkene isomerization and regioselective hydroformylation. A remarkable turnover frequency of 118 h$^{-1}$ was observed.

## Discussion

The above results clearly show that phosphabenzenes are an emerging class of phosphorus-based ligands with a great



0947-6539/01/0714-3114 $ 17.50+.50/0 *Chem. Eur. J.* **2001**, *7*, No. 14

potential for use in homogenous catalysis. They can easily be prepared by condensation of pyrylium salts with $PH_3$ or a synthetic equivalent thereof. Although both $\eta^1$ and $\eta^6$ coordination modes have been observed in transition metal complexes of phosphinines,[15] the preferred binding mode of the phosphabenzenes investigated in this study is the $\eta^1$ coordination toward a rhodium(I) center. The electronic ligand properties of phosphabenzenes could be estimated from the CO-stretching frequency of the corresponding *trans*-[(phosphinine)$_2$RhCl(CO)] complexes. Electronically, the phosphinines resemble phosphite ligands; however, the π-acceptor property is somewhat reduced. Nevertheless, phosphabenzene rhodium(I) complexes have been identified as extremely active and robust hydroformylation catalysts. Hydroformylation experiments have shown that for this class of catalysts, a careful catalyst-preformation procedure is necessary in order to transfer all the rhodium centers into catalytically active species. This may be due to the reduced donor capability of the phosphinine, which may allow the formation of nonactive rhodium-carbonyl clusters under syngas pressure. Extensive hydroformylation experiments under several reaction conditions and with different phosphinine ligands have revealed some interesting trends. Thus, the optimal ligand to rhodium ratio seems to be in the range of 20:1. This ratio seems efficient for transferring all rhodium centers into catalytically active phosphinine complexes. Additionally, this ligand to rhodium ratio allows a high rate for hydroformylation to be combined with a moderate isomerization activity.

Studies on the influence of sterics and electronics in the phosphinine ligand systems have shown a clear trend. Steric effects dominate the catalytic properties of the phosphinine rhodium systems: the larger the *ortho/ortho′* substituents of the phosphinine nucleus, the higher the hydroformylation activity of the corresponding rhodium catalyst. Concomitant with an increase of the hydroformylation rate is an increase in the isomerization rate, with ligand **8** showing maximum activity. Thus, turnover frequencies of up to 45370 $h^{-1}$ for the hydroformylation of oct-1-ene could be reached.

The hydroformylation of more highly substituted alkene substrates with the most active phosphinine **8**/rhodium catalyst were studied in further investigations. The results have been compared with the standard industrial rhodium/triphenylphosphane catalyst. Thus, for all classes of alkenes, including 1,2-disubstituted, 1,1-disubstituted, and trisubstituted alkenes, the phosphinine catalyst is significantly more active. As expected, the reactivity difference between the two catalyst systems becomes larger with increasing alkene substitution. The most striking example is the hydroformylation of a tetrasubstituted alkene, tetramethylethylene. Whereas the triphenylphosphane catalyst did not give any detectable product at all, the phosphinine catalyst consumed this substrate with a turnover frequency of 118 $h^{-1}$.

For reactions of more highly substituted alkenes, the rate determining step has been shown to be early in the catalytic cycle and may be either the alkene coordination or insertion.[42] This is also true for the phosphinine **8**/rhodium catalyst, as reflected in the clean, first-order kinetics upon hydroformylation of cyclohexene. In situ pressure NMR studies have been carried out in order to understand why the rate determining alkene coordination/insertion is accelerated for the phosphinine/rhodium systems. Although experiments with rhodium complexes did not allow the detection of the expected trigonal bipyramidal hydrido complex **26** (Figure 2), such a species could be identified in the case of the more stable iridium(I) system. NMR experiments indicate that only one phosphinine ligand is coordinated to the transition metal center. This situation is similar to that of the bulky phosphite rhodium catalysts.[39] Hence, as in the case of the bulky phosphite ligands, the reasons for the high catalyst activity may be attributed to the formation of a monoligand rhodium species. Such a species should have a larger accessible space compared with the $[HRh(CO)_2(PPh_3)_2]$ system. Hence, the energy barrier for coordination and hydrometallation of a sterically more demanding alkene should be reduced; this is reflected well in the experimental results. Furthermore, in the case of oct-1-ene hydroformylation, the larger accessible space at the rhodium center may allow a more facile reaction to branched species; this may explain the rather modest linearities observed experimentally. Additionally, one may speculate that in a monophosphinine rhodium species, the dissociation of a CO ligand should be easier for electronic reasons. This would induce low coordination numbers and could explain the high tendency of phosphinine rhodium catalysts toward alkene isomerization.

## Conclusion

This study has introduced phosphabenzene/rhodium catalysts as powerful catalysts for the hydroformylation of terminal and, in particular, internal olefins. The catalyst activity is based on the formation of a monoligand metal species, which accounts for the higher rates of hydroformylation and isomerization. Further studies will have to focus on the design of chelating phosphinine ligands to provide active and regioselective hydroformylation catalysts. Experiments to evaluate the full potential of phosphinines as ligands in homogenous late transition metal catalysis are underway.

## Experimental Section

**General**: Reactions were performed in flame-dried glassware either under argon (purity > 99.998 %) or under nitrogen. The solvents were dried by standard procedures, distilled, and stored under nitrogen. All temperatures quoted are uncorrected. $^1$H, $^{13}$C, and $^{31}$P NMR spectra were taken on a Bruker ARX-200, Bruker AC-300, Bruker DRX-400, and Bruker AMX-500 with TMS, chloroform, or benzene as internal standards. For $^{31}$P NMR spectra, 85 % $H_3PO_4$ was used as the external standard. IR spectroscopy: FTIR-510 (Nicolet); mass spectrometry: MAT CH7 (Varian), ZAB2F (Vakuum Generators), and JMS700 (JOEL). Melting points were measured on apparatus by Dr. Tottoli (Büchi). Elemental analyses: CHN rapid analyzer (Heraeus), Vario EL (Analysensysteme GmbH). Flash chromatography: Silica gel Si 60, Merck, Darmstadt, 40–63 μm. Analytical gas chromatography was performed at "Sichromate" (Siemens) and HP 5880A with integrator (Hewlett Packard) employing a column of type OV1, 25 m × 0.25 mm (Hewlett Packard). Hydroformylation reactions were performed in a 100 mL stainless-steel autoclave equipped with a sampling device and gas transfer stirrer (Premex, Switzerland). The stirrer engine was a "Eurodigi-visk" (Ika). A thermostat, type CC301 (Huber), filled with

synthetic oil served as the heating device. In all hydroformylation experiments, the autoclave was connected to a gas reservoir that kept the $CO/H_2$ gas pressure constant throughout the reaction. Gases: Premixed carbon monoxide 1.8 (98%), hydrogen 3.0 (99.9%) in a ratio of 1:1 (Messer-Griesheim).

The following compounds were prepared by literature procedures: chalkone,[44] 2,4,6-triphenylpyrylium tetrafluoroborate,[22] tris(trimethylsilyl)phosphine,[45] and 2,2-dimethylpropylidine phosphane,[45]

**Benzylidene-2-acetonaphton**: Activated barium hydroxide[23] (1.0 g, 5.8 mmol) and benzaldehyde (9.34 g, 88.0 mmol) were added successively to a solution of 2-acetylnaphthalin (10.0 g, 58.8 mmol) in ethanol (80 mL). The reaction mixture was heated under reflux for 2.5 h. After cooling to RT, a precipitate formed which was collected by filtration, then washed with water ($3 \times 5$ mL) and ethanol ($2 \times 5$ mL). The residue was dried in vacuo to give benzylidene-2-acetophenone as pale yellow crystals. Yield: 14.4 g, 95%, m.p. 103 °C (ref. [46], 105 °C); $^1$H NMR (200 MHz, $CDCl_3$): $\delta = 7.43-7.47$ (m, 3H), 7.56–7.62 (m, 2H), 7.65–7.74 (m, 3H), 7.86–8.02 (m, 4H), 8.12 (dd, $J(H,H) = 8.74$, 1.76 Hz, 1H), 8.55 (s, 1H); $^{13}$C NMR (50.33 MHz, $CDCl_3$): $\delta = 122.0$, 124.4, 126.7, 127.8, 128.3 (2C), 128.5 (2 signals), 128.9 (2C), 129.5, 129.9, 130.5, 132.5, 134.9, 135.4, 135.5, 144.7, 190.2. Analytical data correspond to those reported previously.[46]

**4-Trifluormethylbenzylidene acetophenone**: 4-Trifluoromethyl benzaldehyde (5.0 g, 28.7 mmol) was added at RT to a solution of acetophenone (2.87 g, 23.9 mmol) and activated barium hydroxide (200 mg, 1.2 mmol) in ethanol (20 mL). After the solution had been stirred magnetically for 5 min at RT, a yellow precipitate formed, which was collected by filtration then washed with water ($2 \times 2$ mL) and ethanol ($2 \times 1$ mL), and dried in vacuo to give the product as yellow crystals. Yield: 6.2 g, 94%; m.p. 124 °C (ref. [47], 125 °C); $^1$H NMR (300 MHz, $CDCl_3$): $\delta = 7.41-7.77$ (m, 9H), 8.03 (dd, $J(H,H) = 6.7$, 1.8 Hz, 2H); $^{13}$C NMR ($CDCl_3$, 50.33 MHz): $\delta = 124.2$, 125.8 (q, $^3J(C,F) = 3.7$ Hz, 2C), 128.6 (2 signals, each 2C), 128.7, 129.3 (q, $^1J(C,F) = 285$ Hz), 131.5, 133.1 (2C), 137.7, 138.2, 189.9; the signal for *C*-$CF_3$ could not be detected. $^{19}$F NMR ($CDCl_3$, 188 MHz): $\delta = -63.3$; elemental analysis calcd (%) for $C_{16}H_{11}F_3O$ (276.3): C 69.57, H 4.01; found C 69.44, H 4.12.

**4-Methoxybenzylidene acetophenone**: 4-Methoxybenzaldehyde (12.5 g, 91.6 mmol) was added at RT to a solution of acetophenone (10.0 g, 83.2 mmol) and activated barium hydroxide (300 mg, 1.8 mmol) in ethanol (40 mL). The reaction mixture was heated under reflux for 6 h. After cooling to RT, the solvent was reduced in vacuo to a volume of 30 mL. Pouring this mixture into vigorously stirred petroleum ether (50 mL) provided a precipitate, which was collected by filtration. Drying in vacuo provided the product as a pale yellow powder. Yield: 9.5 g, 48%; m.p. 70 °C (ref. [48], 72 °C); $^1$H NMR (300 MHz, $CDCl_3$): $\delta = 3.81$ (s, 3H; $OCH_3$), 6.90 (dt, $^3J(H,H) = 8.8$ Hz, $^4J(H,H) = 2.9$ Hz, 2H), 7.41 (d, $^3J(H,H) = 15.6$ Hz, 1H), 7.44–7.60 (m, 5H; Ph), 7.78 (d, $^3J(H,H) = 15.6$ Hz, 1H), 8.01 (dt, $^3J(H,H) = 6.9$ Hz, $^4J(H,H) = 2.1$ Hz, 2H); $^{13}$C NMR ($CDCl_3$, 50.33 MHz): $\delta = 55.3$, 114.3 (2C), 119.7, 127.5, 128.3 (2C), 128.4 (2C), 130.1 (2C), 132.4, 138.4, 144.5, 161.6, 190.4; elemental analysis calcd (%) for $C_{16}H_{14}O_2$ (238.3): C 80.65, H 5.92; found C 80.46, H 6.11.

**Pyrylium Salts**

*2,6-Dimethyl-4-phenylprylium tetrafluoroborate*:[24] $\alpha$-Methylstyrene (28.4 g, 240 mmol) was added to a solution of tetrafluoroboric acid (54% in diethyl ether, 21.1 g, 240 mmol) in acetic anhydride (200 mL) at 0 °C and the reaction mixture was stirred for 2 h. After standing overnight at RT, the reaction mixture was poured into ether (400 mL). A precipitate formed which was collected by filtration. Recrystallization from hot water (100 mL) gave the product as yellow crystals. Yield: 16.5 g, 25%; m.p. 196 °C; $^1$H NMR (200 MHz, trifluoroacetic acid (TFA)/$CDCl_3$): $\delta = 2.96$ (s, 6H; $CH_3$), 7.62–7.72 (m, 2H; ArH), 7.75–7.84 (m, 1H; ArH), 7.98–8.05 (m, 2H; ArH), 8.07 (s, 2H; C3-H); $^{13}$C NMR (TFA/$CDCl_3$, 50.33 MHz): $\delta = 20.9$ (2C), 118.3 (C3, 2C), 129.7 (2C), 130.7, 131.6 (2C), 136.5, 168.3 (C4), 178.7 (C2, 2C); elemental analysis calcd (%) for $C_{13}H_{13}BF_4O$ (199.1): C 57.39, H 4.82; found C 57.39, H 4.93.

*2,6-Diisopropyl-4-phenylpyrylium tetrafluoroborate*: $\alpha$-methylstyrene (14.2 g, 120 mmol) was added slowly at 0 °C to a solution of tetrafluoroboric acid (54% in diethyl ether, 20.1 g, 120 mmol) in isobutyric anhydride (100 mL). The reaction mixture was stirred for 1 h at RT and additional 5 h at reflux. After cooling the mixture to RT, the precipitated solid was collected by filtration. After washing with cold ether (20 mL) the residue was recrystallized from hot ether (50 mL) to give the pyrylium salt as a beige solid. Yield: 10.1 g, 26%; m.p. 178 °C; $^1$H NMR (300 MHz, $CDCl_3$): $\delta = 1.47$ (d, $^3J(H,H) = 7.0$ Hz, 12H; $CH_3$), 3.56 (sept, $^3J(H,H) = 7.0$ Hz, 2H; CH), 7.56 (t, $^3J(H,H) = 7$ Hz, 2H; ArH), 7.66 (tt, $^3J(H,H) = 7$ Hz, $^4J(H,H) = 2$ Hz, 1H; ArH), 8.11 (dd, $^3J(H,H) = 7$ Hz, $^4J(H,H) = 2$ Hz, 2H; ArH), 8.11 (s, 2H; C4-H); $^{13}$C NMR ($CDCl_3$, 75.47 MHz): $\delta = 20.1$ (4C), 34.5 (2C), 116.5 (C4, 2C), 129.8 (2C), 130.1 (2C), 132.2, 135.2, 167.8 (C5), 184.8 (C3, 2C); elemental analysis calcd (%) for $C_{17}H_{21}BF_4O$ (328.2): C 62.22, H 6.45; found C 62.25, H 6.65.

*6-Methyl-2,4-diphenylpyrylium tetrafluoroborate*: In analogy to a known procedure,[49] the pyrylium salt was obtained from borontrifluoride etherate (22.2 g, 327 mmol), acetophenone (16.0 g, 133 mmol), and acetic anhydride (14.1 g, 138 mmol) as yellow crystals. Yield: 7.9 g, 35%; m.p. 248 °C; $^1$H NMR (200 MHz, TFA): $\delta = 3.19$ (s, 3H; $CH_3$), 7.78–7.97 (m, 6H; ArH), 8.17–8.27 (m, 3H; ArH), 8.36 (d, $J(H,H) = 1.2$ Hz, 1H; ArH), 8.40 (s, 1H), 8.72 (s, 1H); $^{13}$C NMR (TFA, 50.33 MHz): $\delta = 22.8$, 116.9, 120.7, 130.8, 131.0 (2C), 131.7 (2C), 133.0 (2C), 133.2 (2C), 135.0, 138.9, 139.0, 171.0, 176.4, 179.8; elemental analysis calcd (%) for $C_{18}H_{15}BF_4O$ (334.11): C 64.71, H 4.53; found C 64.74, H 4.53.

**General procedure for the preparation of 2,4,6 aryl-substituted pyrylium salts**:[22] Tetrafluoroboric acid (52% ethereal solution, 2.2 equiv) was added at 70 °C within 2 min to a solution of the corresponding chalcone derivative (2.2 equiv) and acetyl derivative (1 equiv) in 1,2-dichloroethane. The reaction mixture was heated under reflux for 4 h, then allowed to cool to RT; this was followed by the addition of a threefold amount of ether. An oil formed which was separated and recrystallized from hot ethanol.

*2-(2-Naphthyl)-4,6-diphenylpyrylium tetrafluoroborate*: The pyrylium salt was obtained from chalcone (5.00 g, 24.0 mmol), 2-acetonaphthone (2.04 g, 12.0 mmol), and tetrafluoroboric acid (52% in ether, 4.68 g, 28.8 mmol) in 1,2-dichloroethane (20 mL) as orange crystals. Yield: 7.61 g, 57%; m.p. 254 °C; $^1$H NMR (300 MHz, TFA/$CDCl_3$): $\delta = 7.34-7.42$ (m, 1H), 7.50–7.75 (m, 8H), 7.80–8.20 (m, 7H), 8.25 (s, 1H), 8.47 (s, 1H), 8.69 (s, 1H); $^{13}$C NMR (TFA/$CDCl_3$, 75.47 MHz): $\delta = 113.8$, 114.3, 122.0, 125.2, 127.9, 128.2 (two signals), 128.7 (2C), 129.0 (2C), 129.3 (two signals), 130.0 (2C), 130.3, 130.7 (2C), 131.3, 132.0, 132.7, 135.7 (two signals), 136.1, 165.5, 170.1, 170.3; FAB$^+$/HR ($C_{25}H_{15}F_6O$): calcd 359.1436; found 359.1453.

*2,6-Di-(2-naphthyl)-4-phenylpyrylium tetrafluoroborate*: The pyrylium salt was obtained as orange crystals from 1-(2-naphthyl)-3-phenylpropenone (7.00 g, 27.1 mmol), 2-acetonaphthone (2.31 g, 13.6 mmol), and tetrafluoroboric acid (52% in ether, 4.85 g, 29.8 mmol) in 1,2-dichloroethane (50 mL). Yield: 1.97 g, 30%; m.p. 254 °C; $^1$H NMR (300 MHz, [D$_6$]acetone): $\delta = 7.77-7.95$ (m, 7H), 8.18 (d, $J(H,H) = 8.0$ Hz, 2H), 8.34 (d, $J(H,H) = 8.1$ Hz, 2H), 8.36 (d, $J(H,H) = 8.7$ Hz, 2H), 8.64 (dt, $J(H,H) = 6.2$ Hz, 1.4 Hz, 2H), 8.74 (dd, $J(H,H) = 8.0$ Hz, 2.0 Hz, 2H), 9.36 (s, 2H), 9.43 (d, $J(H,H) = 2.0$ Hz, 2H); $^{13}$C NMR (TFA/$CDCl_3$, 75.47 MHz): $\delta = 115.1$ (C2, 2C), 123.2 (2C), 126.8 (2C), 129.9 (2C), 130.1, 130.4 (2C), 130.7 (2C), 131.8 (2C), 132.1 (2C), 132.3 (2C), 132.5 (2C), 132.7 (2C), 132.9 (2C), 134.8, 138.0, 138.5, 167.0 (C-3), 171.9 (C-1, 2C).

*4-[4-(Trifluormethyl)phenyl]-2,6-diphenylpyrylium tetrafluoroborate*: The pyrylium salt was obtained as yellow crystals from 1-phenyl-3-(4-trifluoromethylphenyl)propenone (3.00 g, 10.9 mmol), 2-acetophenone (0.65 g, 5.43 mmol), and tetrafluoroboric acid (52% in ether, 1.77 g, 10.9 mmol) in 1,2-dichloroethane (15 mL). Yield: 0.9 g, 36%; m.p. 247 °C; $^1$H NMR (300 MHz, TFA/$CDCl_3$): $\delta = 7.40-7.96$ (m, all H); $^{13}$C NMR (TFA/$CDCl_3$, 75.47 MHz): $\delta = 115.5$ (2C), 124.2 (q, $^1J(C,F) = 270$ Hz, $CF_3$), 126.3 (q, $^3J(C,F) = 3.8$ Hz, 2C), 128.8, 129.4 (4C), 129.5 (2C), 129.7 (4C), 131.0 (2C), 133.7 (q, $^2J(C,F) = 33.0$ Hz), 135.3 (2C), 167.0, 173.0 (2C); FAB$^+$/HR ($C_{24}H_{16}F_3O$): calcd 377.1153; found 377.1153.

*2-[3,5-Bis(trifluoromethyl)phenyl]-4,6-diphenylpyrylium tetrafluoroborate*: The pyrylium salt was obtained as yellow crystals from 3,5-bis(trifluoromethyl)acetophenone (5.00 g, 19.5 mmol), chalcone (8.13 g, 39.0 mmol), and tetrafluoroboric acid (52% in ether, 6.10 g, 39.0 mmol) in 1,2-dichloroethane (10 mL). Yield: 6.50 g, 62%; m.p. 252 °C; $^1$H NMR (300 MHz, $CDCl_3$): $\delta = 7.62-7.88$ (m, 7H), 8.11–8.28 (m, 5H), 8.62 (d, $J(H,H) = 1.6$ Hz, 1H), 8.64 (s, 1H), 8.67 (d, $J(H,H) = 1.6$ Hz, 1H); $^{13}$C NMR (TFA, 75.47 MHz): $\delta = 117.6$, 117.8, 124.6 (q, $^1J(C,F) = 272$ Hz, 2$CF_3$), 130.1 (2C), 130.4 (2C), 130.7 (2C), 131.1 (2C), 131.5, 132.2, 132.5, 133.0, 134.3, 136.7 (q, $^2J(C,F) = 35$ Hz, 2C), 138.7, 138.8, 169.8, 170.8, 175.7; FAB$^+$/HR ($C_{25}H_{15}F_6O$): calcd 445.1027; found 445.1009; elemental analysis calcd (%) for $C_{25}H_{15}BF_{10}O$ (532.18): C 56.41, H 2.84; found C 56.04, H 2.92.



0947-6539/01/0714-3116 $ 17.50+.50/0 *Chem. Eur. J.* **2001**, *7*, No. 14

*2-[3,5-Bis(trifluormethyl)phenyl]-4-(4-trifluormethylphenyl)-6-phenylpyrylium tetrafluoroborate*: The pyrylium salt was obtained as yellow crystals from 1-phenyl-3-(4-trifluoromethylphenyl)propenone (6.90 g, 25.0 mmol), 3,5-bis(trifluoromethyl)acetophenone (3.20 g, 12.5 mmol), and tetrafluoroboric acid (52% in ether, 4.22 g, 25.0 mmol) in 1,2-dichloroethane (25 mL). Yield: 1.60 g, 22%; m.p. 242 °C; $^1$H NMR (300 MHz, TFA/$CDCl_3$): $\delta$ = 7.67–7.76 (m, 3H), 7.80–7.90 (m, 3H), 8.18–8.30 (m, 5H), 8.62–8.73 (m, 3H); $^{13}$C NMR (TFA/$CDCl_3$, 75.47 MHz): $\delta$ = 117.1, 117.4, 127.2 (m, 2C), 127.9, 128.2 (2C), 128.6 (2C), 129.0, 129.8, 130.5, 130.6, 134.1 (q, $^2J$(C,F) = 33 Hz), 135.6, 136.5, 137.1, 166.8, 168.0, 173.7 (signals for $CF_3$ groups could not be detected because of low intensity); $^{19}$F NMR (188 MHz, $CDCl_3$): $\delta$ = –64.0, –64.2, –64.3; FAB$^+$/HR ($C_{26}H_{14}F_9O$): calcd 513.0901; found 513.0921.

*2,6-Diphenyl-4-(4-methoxyphenyl)-pyrylium tetrafluoroborate*: The pyrylium salt was obtained as yellow crystals from 1-phenyl-3-(4-methoxyphenyl)propenone (9.50 g, 41.9 mmol), acetophenone (2.52 g, 21.0 mmol), and tetrafluoroboric acid (52% in ether, 6.90 g, 42.0 mmol) in 1,2-dichloroethane (70 mL). Yield: 3.30 g, 37%; m.p. 233 °C; $^1$H NMR (200 MHz, TFA/$CDCl_3$): $\delta$ = 4.06 (s, 3H; $OCH_3$), 7.28 (dd, $J$(H,H) = 4.0 Hz, 1.7 Hz, 2H), 7.32–7.90 (m, 6H), 8.21–8.37 (m, 6H), 8.48 (s, 2H); $^{13}$C NMR (TFA/$CDCl_3$, 50.33 MHz): $\delta$ = 56.2, 112.6 (2C), 116.8 (2C), 123.1, 128.2 (4C), 128.8 (2C), 130.7 (4C), 132.3 (2C), 136.1 (2C), 165.3, 167.7, 170.8 (2C); elemental analysis calcd (%) for $C_{24}H_{19}BF_4O_2$ (426.21): C 67.63, H 4.49; found C 67.28, H 4.32.

*2-(2-Methoxyphenyl)-4,6-diphenyl-pyrylium tetrafluoroborate*: The pyrylium salt was obtained as yellow crystals from 2-methoxyacetophenone (8.00 g, 53.2 mmol), chalcone (22.2 g, 106 mmol), and tetrafluoroboric acid (52% in ether, 18.0 g, 106 mmol) in 1,2-dichloroethane (20 mL). Yield: 13.2 g, 58%; m.p. 168 °C; $^1$H NMR (300 MHz, $CDCl_3$): $\delta$ = 4.04 (s, 3H; $OCH_3$), 7.20 (t, $J$(H,H) = 7.6 Hz, 1H), 7.25 (d, $J$(H,H) = 8.5 Hz, 1H), 7.50–7.60 (m, 7H), 8.06 (dd, $J$(H,H) = 8.0 Hz, 1.5 Hz, 1H), 8.11–8.16 (m, 2H), 8.22–8.28 (m, 2H), 8.48 (d, $J$(H,H) = 1.5 Hz, 1H), 8.66 (d, $J$(H,H) = 1.5 Hz, 1H); $^{13}$C NMR ($CDCl_3$, 75.47 MHz): $\delta$ = 56.5, 112.9, 113.9, 116.9, 118.0, 122.2, 128.0, 128.3 (2C), 128.4, 129.5 (2C), 130.0 (2C), 130.5 (2C), 132.2, 135.0, 135.1, 137.2, 159.7, 165.3, 168.4, 170.1; elemental analysis calcd (%) for $C_{24}H_{19}BF_4O_2$ (426.20): C 67.63, H 4.49; found C 67.38, H 4.67.

*2-(3-Methoxyphenyl)-4,6-diphenyl-pyrylium tetrafluoroborate*: The pyrylium salt was obtained as yellow crystals from 3-methoxyacetophenone (15.0 g, 99.9 mmol), chalcone (41.6 g, 200 mmol), and tetrafluoroboric acid (52% in ether, 33.7 g, 200 mmol) in 1,2-dichloroethane (40 mL). Yield: 41.6 g, 57%; m.p. 181 °C; $^1$H NMR (300 MHz, TFA/$CDCl_3$): $\delta$ = 3.96 (s, 3H; $OCH_3$), 7.60–7.90 (m, 10H), 8.10–8.16 (m, 2H), 8.24–8.28 (m, 2H), 8.48 (d, $J$(H,H) = 1.5 Hz, 1H), 8.51 (d, $J$(H,H) = 1.5 Hz, 1H); $^{13}$C NMR (TFA/$CDCl_3$, 75.47 MHz): $\delta$ = 55.9, 114.7, 114.9, 121.0, 121.4, 128.3, 129.2 (2C), 129.4(2C), 129.6(2C), 129.7(2C), 130.4, 130.5, 131.7, 132.4, 136.0, 136.1, 160.7, 167.0, 170.9, 171.3.

**8-(2-Naphthyl)-10,11-diphenyl-11*H*-benzo[4,5]indeno[1,2-*b*]pyrylium tetrafluoroborate 16**: Tetrafluoroboric acid (52% ethereal solution, 3.1 g, 19.4 mmol) was added within 2 min to a solution of 1-(2-naphtyl)-3-phenylpropenone (5.00 g, 19.4 mmol) in 1,2-dichloroethane (15 mL) at 70 °C. The reaction mixture was heated to reflux for 4 h, then allowed to cool to RT and poured into ether (45 mL). An oil precipitated which was separated and recrystallized from hot ethanol to give the pyrylium salt **16** as yellow crystals. Yield: 3.20 g, 28%; m.p. 224 °C; $^1$H NMR (300 MHz, TFA/$CDCl_3$): $\delta$ = 5.89 (s, 1H; C*H*Ph), 7.38–7.46 (m, 4H), 7.55 (s, 1H), 7.57 (s, 2H), 7.60–7.80 (m, 3H), 7.88 (d, $J$ = 8.1 Hz, 1H), 7.91–7.99 (m, 5H), 8.00–8.10 (m, 2H), 8.12 (d, $J$(H,H) = 1.1 Hz, 2H), 8.24 (dd, $J$(H,H) = 12.8 Hz, $J$ = 8.7 Hz, 1H), 8.35 (s, 2H), 8.77 (s, 1H); $^{13}$C NMR (75.47 MHz, TFA/$CDCl_3$): $\delta$ = 51.0 (*C*HPh), 115.7, 117.4, 121.8, 125.2, 125.4 (two signals, 2C each), 126.2, 128.0, 128.1 (two signals, 2C each), 128.2, 128.3, 128.4, 128.6, 129.0, 129.2, 129.5, 129.9, 130.1, 130.6, 131.5, 131.7, 132.6, 132.9, 133.15, 133.25, 136.3, 137.8, 138.5, 154.7, 161.4, 167.4, 174.5; FAB$^+$/HR ($C_{38}H_{25}O$): calcd 497.1905; found 497.1903.

**2,6-Bis(2,4-dimethylphenyl)-4-phenylpyrylium tetrafluoroborate**:[21] Tetrafluoroboric acid (54% ethereal solution, 606 g, 3.7 mmol) was added slowly at 80 °C to a solution of benzaldehyde (271 g, 2.6 mmol) and 2,4-dimethylacetophenone (542 g, 3.7 mol) in 1,2-dichloroethane. After stirring for a further 4 h at this temperature, the reaction mixture was allowed to cool to RT. The volatile components were removed in vacuo, and the residue was treated with a toluene/water mixture (1:1). The precipitated orange-yellow solid was collected by filtration, then washed with water and toluene, and dried in vacuo. Recrystallization from hot methanol/dichloromethane provided the pyrylium salt as a bright yellow solid. Yield: 180 g, 32%; m.p. 201 °C; $^1$H NMR (200 MHz, $CDCl_3$): $\delta$ = 2.43 (s, 6H; $CH_3$), 2.57 (s, 6H; $CH_3$), 7.25 (s, 3H), 7.30 (s, 1H), 7.58–7.73 (m, 3H), 7.82 (d, $J$(H,H) = 8.0 Hz, 2H), 8.08 (dd, $J$(H,H) = 8.0 Hz, 1.8 Hz, 2H), 8.20 (d, $J$(H,H) = 9.4 Hz, 2H); $^{13}$C NMR (50.34 MHz, $CDCl_3$): $\delta$ = 21.0, 21.6, 118.0, 126.3, 128.4, 129.3, 130.3, 131.3, 132.8, 133.5, 135.1, 138.4, 145.7, 165.8, 173.8; elemental analysis calcd (%) for $C_{27}H_{25}BF_4O$ (452.29): calcd C 71.70, H 5.57; found C 71.69, H 5.74.

**General procedure for the preparation of phosphabenzenes**

*From pyrylium salts and tris(trimethylsilyl)phosphane (Method A)*:[19] Tris(trimethylsilyl)phosphane (2–2.5 equiv) was added dropwise at RT to a magnetically stirred solution of the corresponding pyrylium salt (1 equiv) in acetonitrile. The resulting black reaction mixture was heated under reflux for 5 h. After cooling to RT, the solvent was removed in vacuo. The residue was dissolved in $CH_2Cl_2$ and an appropriate amount of silica gel was added (0.5 g mmol$^{-1}$). Evaporation of the solvent was followed by flash chromatography with petroleum ether/ethyl acetate (19:1) to give the corresponding phosphabenzene as a colorless to pale yellow solid or oil.

*From pyrylium salts and phosphane (Method B)*:[21] A solution of the corresponding pyrylium salt in a suitable solvent was placed in an autoclave (material: HC). In some cases hydrogen bromide was added as a catalyst. (It was later found that the addition of the acid catalyst is not essential.) The autoclave was pressurized with phosphane gas (5 bar) at room temperature, then the reaction mixture was heated to 110 °C with vigorous mechanical stirring. When the reaction temperature was reached, the phosphane pressure was increased to 30 bar. After 4 h the autoclave was cooled to room temperature, depressurized, and phosphane traces were removed by flushing with nitrogen. The reaction mixture was concentrated, then filtered. The remaining solid was washed with the original solvent, dissolved in toluene and subsequently washed with several portions of water until the water phase was neutral. Toluene was removed in vacuo, and the residue was washed with pentane to yield pure phosphabenzene. If necessary further purification could be achieved by recrystallization.

**2,6-Dimethyl-4-phenylphosphinine (1)**:[50] Phosphinine **1** was obtained as a colorless solid according to method A from the corresponding pyrylium salt (5 g, 18.4 mmol) and P(TMS)$_3$ (9.20 g, 36.8 mmol) in acetonitrile (50 mL). Yield: 876 mg, 24%; m.p. 61 °C; $^1$H NMR (200 MHz, $CDCl_3$): $\delta$ = 2.74 (d, $^3J$(H,P) = 15.1 Hz, 6H; $CH_3$), 7.32–7.44 (m, 3H), 7.53 (d, $J$ = 7.7 Hz, 2H), 7.71 (d, $J$ = 6.7 Hz, 2H); $^{13}$C NMR (75.47 MHz, $CDCl_3$): $\delta$ = 24.6 (d, $^2J$(C,P) = 35.8 Hz, 2$CH_3$), 127.6 (two signals, 2C each), 128.8, 132.1 (d, $^2J$(C,P) = 13.2 Hz, C3, 2C), 142.3 (d, $^4J$(C,P) = 3.2 Hz), 143.3 (d, $^3J$(C,P) = 15.3 Hz, C4), 168.4 (d, $^1J$(C,P) = 49.6 Hz, C2, 2C); $^{31}$P NMR (81 MHz, $CDCl_3$): $\delta$ = 194.3; elemental analysis calcd (%) for $C_{13}H_{13}P$ (200.20): C 77.98, H 6.55; found C 77.74, H 6.63.

**6-Methyl-2,4-diphenylphosphinine (2)**:[20] Phosphinine **2** was obtained as a colorless solid according to method A from the corresponding pyrylium salt (5.01 g, 15.0 mmol) and P(TMS)$_3$ (11.30 g, 45.0 mmol) in acetonitrile (60 mL). Yield: 1.0 g, 25%; m.p. 76 °C; $^1$H NMR (200 MHz, $CDCl_3$): $\delta$ = 2.83 (d, $^2J$(H,P) = 15.5 Hz, 3H; $CH_3$), 7.45 (m, 6H), 7.65 (d, $J$ = 7.3 Hz, 2H), 7.70 (d, $J$ = 8.0 Hz, 2H), 7.88 (d, $J$ = 7.0 Hz, 1H), 8.06 (d, $J$ = 5.7 Hz, 1H); $^{13}$C NMR (100.62 MHz, $CDCl_3$): $\delta$ = 24.8 (d, $^2J$(C,P) = 37.2 Hz, $CH_3$), 127.5 (2C), 127.7 (two signals), 127.8 (2C), 128.8 (2C), 128.9 (2C), 130.9 (d, $^2J$(C,P) = 12.7 Hz, C3/5), 133.0 (d, $^2J$(C,P) = 12.7 Hz, C3/5), 142.3, 143.5 (d, $^3J$(C,P) = 23.7 Hz), 143.7 (d, $^3J$(C,P) = 14.9 Hz, C4), 168.6 (d, $^1J$(C,P) = 50.6 Hz, C2/6), 171.6 (d, $^1J$(C,P) = 51.2 Hz, C2/6); $^{31}$P NMR (81 MHz, $CDCl_3$): $\delta$ = 189.7; elemental analysis calcd (%) for $C_{18}H_{15}P$ (262.27): C 82.43, H 5.77; found C 82.36, H 5.61.

**2,4,6-Triphenylphosphinine (3)**:[51, 21] According to method A, phosphinine **3** was obtained as a pale yellow solid from the corresponding pyrylium salt (5.00 g, 12.6 mmol) and P(TMS)$_3$ (6.32 g, 25.2 mmol) in acetonitrile (30 mL); yield: 1.5 g, 35%. According to method B, apart from a reaction time was 6 h, phosphinine **3** was obtained as a colorless solid from the corresponding pyrylium salt (20 g, 50 mmol) in *n*-butanol (150 mL) after recrystallization from diethyl ether/methanol. Yield: 12.6 g, 77%; m.p. 173 °C; $^1$H NMR (300 MHz, $CDCl_3$): $\delta$ = 7.38–7.46 (m, 8H), 7.64–7.73 (m, 7H), 8.21 (d, $^3J$(H,P) = 6.0 Hz, 2H; H at C3/5); $^{13}$C NMR (75.47 MHz, $CDCl_3$): $\delta$ = 127.6 (2C), 127.7 (2C), 127.9 (4C), 128.9 (2C), 129.0 (4C), 131.9 (d, $^2J$(C,P) = 12.1 Hz, C3/5, 2C), 142.1, 142.2, 143.3 (d, $^2J$(C,P) =

24.1 Hz, 2C), 144.1 (d, $^3J$(C,P) = 13.7 Hz, C4), 171.7 (d, $^1J$(C,P) = 51.9 Hz, C2/6, 2C); $^{31}$P NMR (81 MHz, $CDCl_3$): $\delta$ = 185.1; elemental analysis calcd (%) for $C_{23}H_{17}P$ (324.34): C 85.17, H 5.28; found C 85.24, H 5.10.

**2-(2-Naphthyl)-4,6-diphenylphosphinine (4)**:[21] According to method A, phosphinine **4** was obtained as an orange solid from the corresponding pyrylium salt (6.50 g, 14.5 mmol) and $P(TMS)_3$ (4.38 g, 17.5 mmol) in acetonitrile (55 mL); yield: 1.8 g, 33%. According to method B, apart from a phosphane pressure of 20 bar at reaction temperature, phosphinine **4** was obtained as a yellow solid from the corresponding pyrylium salt (10 g, 22 mmol) and 1 mL hydrogen bromide in acetic acid (30 wt%) in ethanol (150 mL). Yield: 10 g, 84%; $^1$H NMR (200 MHz, $CDCl_3$): $\delta$ = 7.41 – 7.60 (m, 8H), 7.72 – 7.81 (m, 4H), 7.88 – 8.00 (m, 4H), 8.22 (dd, $^3J$ = 6.0 Hz, $^4J$ = 1.2 Hz, 1H; H4), 8.22 (s, 1H; H8), 8.32 (dd, $^3J$ = 6 Hz, $^4J$ = 1.2 Hz, 1H; H2); $^{13}$C NMR (100.61 MHz, $CDCl_3$): $\delta$ = 126.0, 126.1, 126.2, 126.3, 126.5, 127.7 (2C), 127.8 (2C), 128.0 (2C), 128.4, 128.7, 128.9 (2C), 129.0 (2C), 131.8 (d, $^2J$(C,P) = 12.1 Hz, C3/5), 131.9 (d, $^2J$(C,P) = 12.1 Hz, C3/5), 132.9, 133.7, 140.7 (d, $^2J$(C,P) = 24.0 Hz), 142.2, 143.4 (d, $^2J$(C,P) = 24.0 Hz), 144.2 (d, $^3J$(C,P) = 13.6 Hz, C4), 171.6 (d, $^1J$(C,P) = 51.5 Hz, C2/6), 171.8 (d, $^1J$(C,P) = 51.5 Hz, C2/6); $^{31}$P NMR (162 MHz, $CDCl_3$): $\delta$ = 184.5.

**2,6-Di-(2-naphthyl)-4-phenylphosphinine (5)**:[21] According to method A, phosphinine **5** was obtained as a red-orange solid from the corresponding pyrylium salt (4.00 g, 8.06 mmol) and $P(TMS)_3$ (4.44 g, 17.7 mmol) in acetonitrile (80 mL); yield: 450 mg, 15%. According to method B, phosphinine **5** was obtained as a yellow solid from the corresponding pyrylium salt (2.5 g, 5.0 mmol) and hydrogen bromide in acetic acid (1 mL, 30 wt%) in *n*-butanol (150 mL) after recrystallization from toluene/pentane. Yield: 1.0 g, 47%; m.p. 171 °C; $^1$H NMR (300 MHz, $CD_2Cl_2$): $\delta$ = 7.57 (m, 7H), 7.75 (m, 2H), 7.80 – 7.99 (m, 8H), 8.24 (s, 2H; H5), 8.29 (d, $J$ = 6.0 Hz, 2H); $^{13}$C NMR (125.77 MHz, $CDCl_3$): $\delta$ = 126.0 (d, $J$(C,P) = 12.6 Hz, 2C), 126.3 (2C), 126.4, 126.5 (2C), 127.7 (2C), 127.9 (2C), 128.0 (2C), 128.4 (2C), 128.7 (2C), 129.0 (2C), 132.0 (d, $^2J$(C,P) = 11.3 Hz, C3/5, 2C), 133.0 (2C), 133.7 (2C), 140.6 (d, $^2J$(C,P) = 23.9 Hz, 2C), 142.2, 144.3 (d, $^3J$(C,P) = 13.8 Hz, C4), 171.6 (d, $^1J$(C,P) = 51.5 Hz, C-2/6, 2C); $^{31}$P NMR (81 MHz, $CDCl_3$): $\delta$ = 185.5; HRMS ($C_{31}H_{21}P$): calcd 424.1381; found 424.1380.

**2,6-Diisopropyl-4-phenylphosphinine (6)**: According to method A, phosphinine **6** was obtained as a pale yellow viscous oil from the corresponding pyrylium salt (10.00 g, 30.5 mmol) and $P(TMS)_3$ (19.0 g, 76.0 mmol) in acetonitrile (25 mL). Yield: 2.3 g, 30%; $^1$H NMR (300 MHz, $CDCl_3$): $\delta$ = 1.41 (d, $^3J$(H,H) = 7 Hz, 12H; $CH_3$), 3.31 (sept, $^3J$(H,H) = 7 Hz, 2H; CH), 7.36 – 7.60 (m, 5H; Ph), 7.83 (d, $^3J$(H,P) = 7 Hz, 2H; H4); $^{13}$C NMR (125.77 MHz, $CDCl_3$): $\delta$ = 26.0 (2C), 38.0 (d, $^2J$(C,P) = 29.0 Hz, 2C), 127.5, 127.7 (d, $J$(C,P) = 1.9 Hz, 2C), 128.8 (2C), 130.1 (d, $^3J$(C,P) = 12.2 Hz, C3/5, 2C), 142.9 (d, $^4J$(C,P) = 3.0 Hz), 143.1 (d, $^3J$(C,P) = 16 Hz, C4), 181.6 (d, $^1J$(C,P) = 52.8 Hz, C1/6, 2C); $^{31}$P NMR (81 MHz, $CDCl_3$): $\delta$ = 187.4; elemental analysis calcd (%) for $C_{17}H_{21}P$ (256.31): C 79.66, H 8.26; found C 79.53, H 8.50.

**8-Naphthalin-2-yl-10,11-diphenyl-11*H*-7-phosphabenzo[*a*]fluoren (7)**: According to method A, phosphinine **7** was obtained from the corresponding pyrylium salt (2.90 g, 4.96 mmol) and $P(TMS)_3$ (2.9 g, 11.7 mmol) in

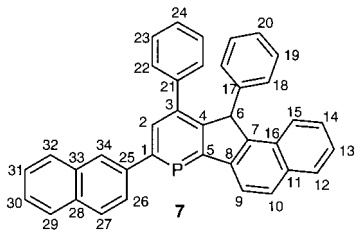

**7**

acetonitrile (20 mL, 1.15 g, 45%) as an orange solid. Assignment of signals is based on $^1J$(C,H), $^{2,3}J$(C,H) and $^3J$(H,H) correlation, and $^{13}$C DEPT NMR experiments. $^1$H NMR (300 MHz, $CDCl_3$): $\delta$ = 5.65 (s, 1H; H6), 6.46 (d, $^3J$(H,H) = 6.8 Hz, 2H; H18), 6.80 – 6.96 (m, 3H; H19, H20), 7.13 (d, $^3J$(H,H) = 8.0 Hz, 2H; H22), 7.20 – 7.39 (m, 5H; H23, H-24, H13+1ArH), 7.42 – 7.50 (m, 2H; H30/32+1 ArH), 7.67 (d, $^3J$(H,H) = 8.2 Hz, 1H; H15), 7.82 – 7.94 (m, 7H; H2, H10, H30/32, H26, + 3 ArH), 8.19 (s, 1H; H34), 8.30 (dd, $^3J$(P,H) = 8.4 Hz, $^4J$(H,H) = 1.5 Hz, 1H; H9); $^{13}$C NMR (125.77 MHz, $CDCl_3$): $\delta$ = 55.9 (C6), 119.3 (d, $^3J$(C,P) = 9.2 Hz, C9), 124.5 (C15), 125.6 (C20), 125.9, 126.0 (C34), 126.1, 126.2, 126.4, 126.6, 127.3 (C24), 127.6, 127.7, 127.9 (C19), 128.2 (C18), 128.4 (C23), 128.5, 128.6 (C22), 129.0, 129.1, 129.9, 132.9 (C28), 133.7 (C33), 134.1 (C16), 134.5 (d, $^2J$(C,P) = 12.2 Hz, C2), 139.2 (C17), 141.0 (d, $^2J$(C,P) = 24.9 Hz, C25), 141.7 (C21), 142.6 (d, $^3J$(C,P) = 14.2 Hz, C3), 142.7 (C7), 143.4 (d, $^2J$(C,P) = 11.2 Hz, C8), 151.7 (d, $^3J$(C,P) = 12.7 Hz, C4), 168.4 (d, $^1J$(C,P) = 48.3 Hz, C1), 169.2 (d, $^1J$(C,P) = 47.8 Hz, C5); $^{31}$P NMR (81 MHz, $CDCl_3$): $\delta$ = 162.7; HRMS ($C_{38}H_{25}P$): calcd 512.1694; found 512.1694.

**2,6-Bis-(2,4-dimethylphenyl)-4-phenylphosphinine (8)**:[21] According to method B, phosphinine **8** was obtained as a colorless solid from the corresponding pyrylium salt (20 g, 44 mmol) in *n*-butanol (150 mL) after recrystallization from diethyl ether/methanol. Yield: 8.9 g, 53%; m.p. 171 °C; $^1$H NMR (200 MHz, $CD_2Cl_2$): $\delta$ = 2.34 (s, 6H; $CH_3$), 2.37 (s, 6H; $CH_3$), 7.04 – 7.16 (m, 4H), 7.18 – 7.28 (m, 2H), 7.30 – 7.50 (m, 3H), 7.65 – 7.68 (m, 2H), 7.93 (d, $^3J$(H,P) = 6.2 Hz, 2H; C3/5-H); $^{13}$C NMR (50.23 MHz, $CDCl_3$): $\delta$ = 20.9 (d, $J$(C,P) = 2.7 Hz), 21.1, 126.5, 127.7 (d, $J$(C,P) = 5.5 Hz), 128.9, 130.2, 130.4, 131.3, 132.7, 132.8 (d, $^2J$(C,P) = 11.0 Hz, C3/5), 134.8 (d, $J$(C,P) = 4.6 Hz), 137.4, 140.4 (d, $^2J$(C,P) = 23.0 Hz), 142.1 (d, $^3J$(C,P) = 13.8 Hz, C4), 172.5 (d, $^1J$(C,P) = 53.9 Hz, C2/6); $^{31}$P NMR (81 MHz, $CDCl_3$): $\delta$ = 194.3; elemental analysis calcd (%) for $C_{27}H_{25}P$ (380.46): C 85.24, H 6.62; found C 84.98, H 6.59.

**4-(4-Methoxyphenyl)-2,6-diphenylphosphinine 9**:[21, 51] According to method A, phosphinine **9** was obtained as a yellow solid from the corresponding pyrylium salt (3.30 g, 7.74 mmol) and $P(TMS)_3$ (3.88 g, 15.5 mmol) in acetonitrile (10 mL); yield: 540 mg, 20%. According to method B, phosphinine **9** was obtained as a pale yellow solid from the corresponding pyrylium salt (13 g, 31 mmol) in *n*-butanol (150 mL). Yield: 4.3 g, 39%; m.p. 104 °C; $^1$H NMR (200 MHz, $C_6D_6$): $\delta$ = 3.44 (s, 3H; $CH_3$), 6.97 (d, $^3J$ = 8.8 Hz, 2H), 7.34 – 7.26 (m, 6H), 7.50 (d, $J$ = 8.5 Hz, 2H), 7.82 (dt, $J$ = 6.5 Hz, 1.5 Hz, 4H), 8.26 (d, $^3J$(H,P) = 5.8 Hz, 2H; C3/5-H); $^{13}$C NMR (50.33 MHz, $C_6D_6$): $\delta$ = 55.3, 115.2 (2C), 127.9 (2C), 128.4 (4C), 128.9 (4C), 129.6 (2C), 132.3 (d, $^2J$(C,P) = 12.4 Hz, C3/5, 2C), 135.4 (d, $^4J$(C,P) = 3.3 Hz), 144.5, 144.5 (d, $^2J$(C,P) = 24.3 Hz, 2C), 160.6 (C11), 172.8 (d, $^1J$(C,P) = 52 Hz, C2/6, 2C); $^{31}$P NMR (81 MHz, $C_6D_6$): $\delta$ = 181.9; elemental analysis calcd (%) for $C_{24}H_{19}OP$ (354.36): C 81.34 H 5.40; found C 81.38, H 5.60.

**4-[4-(Trifluormethyl)phenyl]-2,6-diphenylphosphinine (10)**: According to method A, phosphinine **10** was obtained as a yellow solid from the corresponding pyrylium salt (2.00 g, 4.3 mmol) and $P(TMS)_3$ (2.7 g, 10.7 mmol) in acetonitrile (60 mL). Yield: 680 mg, 51%; $^1$H NMR (200 MHz, $C_6D_6$): $\delta$ = 7.35 – 7.54 (m, 8H), 7.70 (d, $J$ = 8.0 Hz, 2H), 7.91 (dt, $J$ = 8.0 Hz, 1.5 Hz, 4H), 8.17 (d, $^3J$(P,H) = 6.0 Hz, 2H; C3/5-H); $^{13}$C NMR (125.77 MHz, $CDCl_3$): $\delta$ = 124.2 (q, $^1J$(C,F) = 273 Hz, $CF_3$), 125.9 (q, $^3J$(C,F) = 3.8 Hz, 2C), 127.7 (d, $^3J$(C,P) = 12.5 Hz, 4C), 128.10 (2C), 128.15 (2C), 129.0 (4C), 130.0 (q, $^2J$(C,F) = 32.7 Hz), 131.5 (d, $^2J$(C,P) = 11.3 Hz, C3/5, 2C), 142.5 (d, $^3J$(C,P) = 13.7 Hz, C4), 143.1 (d, $^2J$(C,P) = 23.9 Hz, 2C), 145.7, 172.1 (d, $^1J$(C,P) = 52.8 Hz, C2/6, 2C); $^{31}$P NMR (81 MHz, $CDCl_3$): $\delta$ = 189.6; $^{19}$F NMR ($C_6D_6$, 188 MHz): $\delta$ = – 62.4; elemental analysis calcd (%) for $C_{24}H_{16}F_3P$ (392.34): C 73.47 H 4.11; found C 73.20, H 3.85.

**2-[3,5-Bis(trifluormethyl)phenyl]-4,6-diphenylphosphinine (11)**: According to method A, phosphinine **11** was obtained as a yellow solid from the corresponding pyrylium salt (4.00 g, 7.5 mmol) and $P(TMS)_3$ (4.70 g, 18.8 mmol) in acetonitrile (20 mL). Yield: 700 mg, 20%; $^1$H NMR (200 MHz, $CDCl_3$): $\delta$ = 7.42 – 7.55 (m, 6H), 7.68 – 7.76 (m, 4H), 7.94 (s, 1H; H1), 8.16 (s, 3H), 8.27 (d, $^3J$ = 6.2 Hz, 1H; H9); $^{13}$C NMR (125.77 MHz, $CDCl_3$): $\delta$ = 121.5 (m), 123.3 (q, $^1J$(C,F) = 273 Hz, 2$CF_3$), 127.67 (d, $^3J$(C,P) = 11.3 Hz, 2C), 127.72 (m, 2C), 127.8 (2C), 128.4 (2C), 129.1 (2C), 129.2 (2C), 132.1 (d, $^2J$(C,P) = 12.5 Hz, C3/5), 132.3 (q, $^2J$(C,F) = 32.7 Hz, 2C), 132.8 (d, $^2J$(C,P) = 12.5 Hz, C3/5), 141.6, 142.7 (d, $^2J$(C,P) = 23.8 Hz), 144.9 (d, $^3J$(C,P) = 13.8 Hz, C8), 145.4 (d, $^2J$(C,P) = 26.4 Hz), 168.1 (d, $^1J$(C,P) = 52.8 Hz, C2/6), 172.2 (d, $^1J$(C,P) = 52.8 Hz, C2/6); $^{31}$P NMR (202 MHz, $CDCl_3$): $\delta$ = 186.2; HRMS ($C_{25}H_{15}F_6P$): calcd 460.0815 found 460.0812.

**2-[3,5-Bis(trifluormethyl)phenyl]-4-[4-(trifluormethyl)phenyl]-6-phenylphosphinine (12)**: According to method A, phosphinine **12** was obtained as a yellow solid from the corresponding pyrylium salt (1.50 g, 2.5 mmol) and $P(TMS)_3$ (1.60 g, 6.25 mmol) in acetonitrile (20 mL). Yield: 270 mg, 20%; $^1$H NMR (300 MHz, $CDCl_3$): $\delta$ = 7.38 (d, $J$ = 6.0 Hz, 3H), 7.62 (d, $J$ = 6.2 Hz, 1H), 7.68 (s, 5H), 7.84 (s, 1H; H1), 8.04 (s, 3H), 8.12 (d, $J$ =



0947-6539/01/0714-3118 $ 17.50+.50/0 *Chem. Eur. J.* **2001**, *7*, No. 14

6.0 Hz, 1H); $^{13}$C NMR (75.47 MHz, $CDCl_3$): $\delta = 121.8$, 123.3 (q, $^1J(C,F) = 273$ Hz, $2CF_3$), 126.2 (q, $^3J(C,F) = 3.7$ Hz, 2C), 127.6 (2C), 127.7 (2C), 128.2 (2C), 128.6 (2C), 129.2, 130.4 (q, $^2J(C,P) = 32.6$ Hz, C15), 131.8 (d, $^2J(C,P) = 12.3$ Hz, C3/5), 132.4 (q, $^2J(C,F) = 33.5$ Hz, 2C), 132.5 (d, $^2J(C,P) = 11.4$ Hz, C3/5), 142.4 (d, $^2J(C,P) = 24.4$ Hz), 143.3 (d, $^3J(C,P) = 13.7$ Hz, C4), 145.0 (m), 145.3, 168.5 (d, $^1J(C,P) = 53.0$ Hz, C1/6), 172.6 (d, $^1J(C,P) = 52.0$ Hz, C1/6); $^{31}$P NMR (81 MHz, $CDCl_3$): $\delta = 191.5$; $^{19}$F NMR (188 MHz, $CDCl_3$): $\delta = 62.8$, 63.2; ; HRMS ($C_{26}H_{14}F_9P$): calcd 528.0689 found 528.0692.

**2-(2-Methoxyphenyl)-4,6-diphenylphosphinine (13)**:[21] According to method A, phosphinine **13** was obtained as a yellow solid from the corresponding pyrylium salt (10.00 g, 23.5 mmol) and $P(TMS)_3$ (14.70 g, 58.7 mmol) in acetonitrile (30 mL); yield: 3.95 g, 48%. According to method B, phosphinine **13** was obtained as a pale yellow solid from the corresponding pyrylium salt (20 g, 47 mmol) in *n*-butanol (150 mL). Yield: 4.7 g, 28%; m.p. 78 °C; $^1$H NMR (300 MHz, $CDCl_3$): $\delta = 3.83$ (s, 3H; $CH_3$), 7.00–7.11 (m, 2H), 7.34–7.52 (m, 8H), 7.64–7.76 (m, 4H), 8.14–8.20 (m, 2H; H at C3/5); $^{13}$C NMR (75.47 MHz, $CDCl_3$): $\delta = 55.8$, 111.4, 121.0, 127.7, 127.76, 127.84, 128.1, 128.2 (2C), 128.6 (2C), 128.86 (2C), 128.92 (2C), 129.3, 131.4 (d, $^2J(C,P) = 11.7$ Hz, C3/5), 133.9 (d, $^2J(C,P) = 12.1$ Hz, C3/5), 142.3, 142.9 (d, $^3J(C,P) = 13.6$ Hz, C4), 143.6 (d, $^2J(C,P) = 24.9$ Hz), 155.9 (d, $^3J(C,P) = 4.2$ Hz), 168.4 (d, $^1J(C,P) = 52.1$ Hz, C2/6), 171.4 (d, $^1J(C,P) = 53.3$ Hz, C2/6); $^{31}$P NMR (81 MHz, $CDCl_3$): $\delta = 191.8$; elemental analysis calcd (%) for $C_{24}H_{19}OP$ (354.36): C 81.34 H 5.40; found C 81.10, H 5.44.

**2-(3-Methoxyphenyl)-4,6-diphenylphosphinine (14)**:[21] According to method A, phosphinine **14** was obtained as a pale yellow solid from the corresponding pyrylium salt (10.00 g, 23.5 mmol) and $P(TMS)_3$ (11.80 g, 47 mmol) in acetonitrile (100 mL); yield: 2.95 g, 36%. According to method B, phosphinine **14** was obtained as a pale yellow solid from the corresponding pyrylium salt (13 g, 31 mmol) in *n*-butanol (150 mL). Yield: 4.3 g, 39%; m.p. 121 °C; $^1$H NMR (500 MHz, $CDCl_3$): $\delta = 3.87$ (s, 3H; $CH_3$), 6.96 (dd, $J = 7.9$ Hz, 2.4 Hz, 1H), 7.32 (d, $J = 7.7$ Hz, 1H), 7.37–7.42 (m, 3H), 7.46–7.50 (m, 4H), 7.68 (d, $J = 7.3$ Hz, 2H), 7.73 (d, $J = 7.9$ Hz, 2H), 8.17 (d, $J = 5.9$ Hz, 2H); $^{13}$C NMR (75.47 MHz, $CDCl_3$): $\delta = 55.3$, 113.2 (d, $^3J(C,P) = 12.8$ Hz), 113.6, 120.2 (d, $^3J(C,P) = 12.8$ Hz), 127.6 (2C), 127.8 (two signals), 128.0 (2C), 128.9 (2C), 129.0 (2C), 129.9, 131.7 (d, $^2J(C,P) = 11.3$ Hz, C3/5), 131.8 (d, $^2J(C,P) = 11.3$ Hz, C3/5), 142.1 (d, $^4J(C,P) = 3$ Hz), 143.4 (d, $^2J(C,P) = 24.1$ Hz), 144.1 (d, $^3J(C,P) = 13.7$ Hz, C4), 144.8 (d, $^2J(C,P) = 24.9$ Hz), 160.0, 171.6 (d, $^1J(C,P) = 52.8$ Hz, C2/6), 171.8 (d, $^1J(C,P) = 52.1$ Hz, C2/6); $^{31}$P NMR (81 MHz, $CDCl_3$): $\delta = 185.2$; elemental analysis calcd (%) for $C_{24}H_{19}OP$ (354.36): C 81.34 H 5.40; found C 81.40, H 5.46.

**2-*tert*-Butyl-4,6-diphenylphosphinine (15)**: A solution of 4,6-diphenyl-$\alpha$-pyrone **19**[52] (497 mg, 2.0 mmol) and 2,2-dimethylpropylidinphosphane[45] (220 mg, 2.2 mmol) in benzene (3 mL) was heated in a Schlenk pressure vessel to 140 °C for 3 d. After cooling the solution to RT, all volatile components were removed in vacuo, and the residue was purified by flash chromatography with petroleum ether/ethylacetate (19:1) to give phosphinine **15** as a yellow oil. Yield: 330 mg, 54%; $^1$H NMR (300 MHz, $CDCl_3$): $\delta = 1.46$ (d, $^4J(H,P) = 1.5$ Hz, 9H; $C(CH_3)_3$), 7.10–7.28 (m, 6H), 7.48 (m, 2H), 7.68 (m, 2H), 8.03 (dd, $J = 5.8$ Hz, 1.1 Hz, 1H), 8.11 (dd, $J = 6.4$ Hz, 1.1 Hz, 1H); $^{13}$C NMR (75.47 MHz, $CDCl_3$): $\delta = 32.7$ (d, $^3J(C,P) = 12.2$ Hz, $C(CH_3)_3$), 38.7 (d, $^2J(C,P) = 21.1$ Hz, $C(CH_3)_3$), 127.8 (2C), 128.6 (2C), 128.8 (2C), 129.4 (2C), 129.5 (d, $^2J(C,P) = 12.4$ Hz), 130.1 (d, $^2J(C,P) = 12.4$ Hz), 130.8, 131.0, 143.0 (d, $^3J(C,P) = 29.4$ Hz), 143.4 (d, $^3J(C,P) = 14.0$ Hz), 144.2, 170.6 (d, $^1J(C,P) = 52.0$ Hz, C6), 185.3 (d, $^1J(C,P) = 59.3$ Hz, C2); $^{31}$P NMR (81 MHz, $CDCl_3$): $\delta = 187.8$.

**General procedure for the preparation of rhodium(I)-phosphinine complexes**: The corresponding phosphinine (300 μmol) was added slowly to a solution of rhodium dicarbonyl chloride dimer (26.5 mg, 68.2 μmol) in $CH_2Cl_2$ (2 mL). A vigorous gas evolution was observed. After stirring the mixture magnetically for a further hour at RT, the solvent was removed in vacuo to give the rhodium complexes in quantitative yields.

*trans-[Rh{$\eta^1$-($C_{23}H_{17}P$)}$_2$Cl(CO)]* (**22**): Crystals suitable for X-ray analysis were obtained from a concentrated solution of the complex in $CH_2Cl_2$ at RT. $^1$H NMR (400 MHz, $CDCl_3$): $\delta = 7.39–7.48$ (m, 14H), 7.53 (m, 4H), 7.67 (d, $J = 7.9$ Hz, 4H), 7.94 (d, $J = 7.4$ Hz, 8H), 8.25 (pseudo t, $J = 10.2$ Hz, 4H); $^{13}$C NMR (100.61 MHz, $CDCl_3$): $\delta = 127.5$, 128.0, 128.1, 128.2, 128.9, 129.4 (pt, $J = 5.1$ Hz), 135.7, 140.5 (pt, $J = 6.8$ Hz), 141.1 (C4), 141.9 (pt, $J = 11.8$ Hz, C3), 161.7 (ptd, $J = 11.8$ Hz, 3.8 Hz), 181.9 (dt, $^1J(C,Rh) = 64.0$ Hz, $^2J(P,C) = 22.1$ Hz, CO); $^{31}$P NMR (162 MHz, $CDCl_3$): $\delta = 168.9$ (d, $^1J(Rh,P) = 174$ Hz); IR($CH_2Cl_2$): $\tilde{\nu} = 1999\,cm^{-1}$, FAB$^+$/HR ($C_{47}H_{34}ClOP_2Rh$): calcd. 814.0828; found 814.0828.

*X-ray crystal structure analysis of rhodium complex* **22**: $[C_{46}H_{34}ClOP_2Rh] \cdot 0.5\,CH_2Cl_2$, $M_w = 857.51$, triclinic, space group $P\bar{1}$, $a = 1096.6(1)$, $b = 1386.8(1)$, $c = 1430.6(1)$ pm, $\alpha = 79.09(1)$, $\beta = 74.83(1)$, $\gamma = 74.74(1)°$, $U = 2008(3)$ Å$^3$, $D_c = 1.418\,g\,cm^{-3}$ for $Z = 2$, F(000) = 874, $\mu(MoK_\alpha) = 0.674\,mm^{-1}$, $\lambda = 0.71073$ Å, $T = 193(2)$ K, crystal size $0.3 \times 0.3 \times 0.2$ mm. A total of 8182 reflections was collected (Enraf Nonius CAD4) by using $\vartheta/2\theta$ scans in the range $2.3 < \theta < 26°$, 7851 were unique ($R_{int} = 0.0493$). The structure was solved by direct methods. Full-matrix least-squares refinement was based on $F^2$, with all non-hydrogen atoms anisotropic and with hydrogens included in calculated positions with isotropic temperature factors 1.2 times that of the $U_{eq}$ of the atom to which they were bonded. The refinement converged at $R1 = 0.0716$ (for 6686 reflections with $I > 2\sigma(I)$) and $wR2 = 0.2300$ (all data) [$w = (\sigma^2(F_o)^2 + (0.1918P)^2 + 0.6691P)^{-1}$ where $P = (F_o^2 + 2F_c^2)/3$]; final GOF = 1.056; largest peak and hole in the final difference Fourier: 2.26/3.37 e Å$^{-3}$. The programs used were SHELXS-97[53] and SHELXL-97.[54] Crystallographic data (excluding structure factors) have been deposited with the Cambridge Crystallographic Data Centre as supplementary publication no. CCDC-156962. Copies of the data can be obtained free of charge on application to CCDC, 112 Union Road, Cambridge CB2 1EZ, UK (fax: (+44) 1233-336033; e-mail: deposit@ccdc.cam.ac.uk).

*trans-[Rh{$\eta^1$-($C_{31}H_{21}P$)}$_2$Cl(CO)]* (**23**): $^1$H NMR (400 MHz, $CDCl_3$): $\delta = 7.40–7.52$ (m, 18H), 7.71 (d, $J = 8.4$ Hz, 4H), 7.79 (t, $J = 6.8$ Hz, 8H), 8.08 (d, $J = 8.4$ Hz, 4H), 8.34–8.40 (m, 8H); ); $^{13}$C NMR (100.61 MHz, $CDCl_3$): $\delta = 126.9$, 127.0, 128.0, 128.06 (2C), 128.12 (2C), 128.6, 128.7, 128.8, 129.5, 133.5 (d, $J = 19$ Hz), 137.2, 138.7 (pt, $J = 6.5$ Hz), 141.6, 142.7 (t, $J = 11.8$ Hz), 162.6 (m), 181.4 (dt, $^1J(C,Rh) = 65.1$ Hz, $^2J(C,P) = 22.0$ Hz, CO); $^{31}$P NMR (81 MHz, $CDCl_3$): $\delta = 166.8$ (d, $^1J(Rh,P) = 174.2$ Hz); IR($CH_2Cl_2$): $\tilde{\nu} = 1998\,cm^{-1}$.

*trans-[Rh{$\eta^1$-($C_{24}H_{19}OP$)}$_2$Cl(CO)]* (**24**): $^1$H NMR (400 MHz, $CDCl_3$): $\delta = 3.83$ (s, 6H; H9), 7.00 (d, $J = 8.8$ Hz, 4H), 7.34–7.41 (m, 12H), 7.57 (d, $J = 8.8$ Hz, 4H), 7.89 (d, $J = 7.0$ Hz, 8H), 8.16 (t, $J = 10.2$ Hz, 4H); ); $^{13}$C NMR (100.61 MHz, $CDCl_3$): $\delta = 55.4$, 114.5, 128.3, 128.4, 128.8, 129.5 (pt, $J = 5.1$ Hz), 133.7, 135.5, 140.8 (pt, $J = 6.9$ Hz), 141.7 (pt, $J = 11.6$ Hz), 159.9, 161.8 (dpt, $J = 14.4$ Hz, 2.9 Hz), 180.9 (dt, $^1J(Rh,C) = 64.5$ Hz, $^2J(C,P) = 21.6$, CO); $^{31}$P NMR (81 MHz, $CDCl_3$): $\delta = 166.1$ (d, $^1J(Rh,P) = 174.0$ Hz); IR($CH_2Cl_2$): $\tilde{\nu} = 2002\,cm^{-1}$.

*trans-[Rh{$\eta^1$-($C_{24}H_{16}F_3P$)}$_2$Cl(CO)]* (**25**): $^1$H NMR (200 MHz, $CDCl_3$): $\delta = 7.15–8.29$ (m, all H); $^{13}$C NMR (100.61 MHz, $CDCl_3$): $\delta = 122.7$, 125.4, 126.0, 128.0, 128.4, 128.7, 129.4, 135.7, 136.2, 140.4, 144.7, 162.2 (pt, $J = 9.6$ Hz, C1), 180.7 (dt, $^1J(Rh,C) = 65.1$ Hz, $^2J(C,P) = 20.7$ Hz, CO), $^{31}$P NMR (81 MHz, $CDCl_3$): $\delta = 173.8$ (d, $^1J(Rh,P) = 175.0$ Hz); IR($CH_2Cl_2$): $\tilde{\nu} = 2003\,cm^{-1}$.

**Experiments to determine the nature of the catalytically active species**: Under an atmosphere of dry and oxygen-free nitrogen (glove box) [Rh(COD)$_2$OTf] (12.3 mg, 26.3 μmol) and phosphabenzene **8** (20 mg, 52.6 μmol) were dissolved in $CD_2Cl_2$ (1 mL) and transferred into a sapphire NMR pressure vessel. A pressure of 40 bar $CO/H_2$ (1:1) was applied, and the sample was heated for 1 h at 90 °C. After cooling to RT, the sample thus obtained was investigated by $^1$H and $^{31}$P NMR spectroscopy. $^1$H NMR (400 MHz, 25 °C, $CD_2Cl_2$): A RhH signal could not be detected; $^{31}$P NMR (161 MHz, $CD_2Cl_2$): $\delta = 154.5$ (br s). −90 °C: $^{31}$P NMR (161 MHz, $CD_2Cl_2$): $\delta = 146.75$ (d, $^1J(P,Rh) = 140$ Hz, major species), 156.63 (d, $^1J(P,Rh) = 149$ Hz, minor species), ratio major/minor: about 6:1.

Under an atmosphere of dry and oxygen-free nitrogen (glove box), [Ir(CO)$_2$acac] (9.1 mg, 26.3 μmol) and phosphabenzene **8** (20 mg, 52.6 μmol) were dissolved in $CD_2Cl_2$ (1 mL) and transferred into a sapphire NMR pressure vessel. A pressure of 40 bar $CO/H_2$ (1:1) was applied, and the sample was heated for 1 h at 90 °C. After cooling to −90 °C the sample thus obtained was investigated by $^1$H and $^{31}$P NMR spectroscopy. $^1$H NMR (500 MHz, $CD_2Cl_2$): $\delta = -11.83$ (d, $^2J(H,P) = 23.2$ Hz, P-Ir-H); $^{31}$P NMR (202.46 MHz, $CD_2Cl_2$): $\delta = 189.7$ (free phosphinine), 144.3 (s), 143.9(s), ratio: about 2:1:1.

**General procedure for hydroformylation of oct-1-ene**: [Rh(CO)$_2$acac] (3.1 mg, 12.0 μmol) and the appropriate amount of phosphinine (usually 240 μmol) were dissolved in toluene (5 mL) and stirred magnetically for 30 min. Subsequently, oct-1-ene (2.86 g, 25 mmol) was added, and the

resulting solution was transferred into the autoclave. Additional toluene (5 mL) was added, and the autoclave was heated to 90 °C while the mixture was stirred (1000 $min^{-1}$). When the mixture reached this temperature, a $CO/H_2$ (1:1) gas pressure of 10 bar was applied. After 20 h, complete consumption of the starting material was determined by GC analysis and the concentrations ($c_0$) of all ingredients were quantified. The gas pressure was released, followed by immediate and rapid addition of oct-1-ene (5.71 g, 50 mmol). The kinetic experiment was started immediately by readjustment of the gas pressure ($CO/H_2$). Samples were taken from the autoclave through a sample valve at the times indicated and analyzed immediately by GC. Substraction of the initial concentration ($c_0$) provided the kinetic data of the hydroformylation experiment.

**Hydroformylation of cyclohexene**: $[Rh(CO)_2acac]$ (3.1 mg, 12.0 μmol) and the corresponding ligand (20 equiv, 240 μmol) were dissolved in toluene and stirred for 30 min at room temperature. Cyclohexene (4.10 g, 50 mmol) was added, then the reaction mixture was transferred into the autoclave and heated to 90 °C within 15 min. When the mixture reached this temperature, a syngas pressure of 40 bar was applied. The reaction mixture was analyzed by GC with internal standard and correction factors.

**General procedures for the hydroformylation of more highly substituted olefins**: *Variant A*: $[Rh(CO)_2acac]$ and the ligand were dissolved in toluene, and the mixture transferred into the autoclave. A pressure of 3 – 5 bar $CO/H_2$ (1:1) was applied, and the autoclave was heated within 30 min to the corresponding reaction temperature while the mixture was stirred (1000 $min^{-1}$). The olefin was added to the reaction mixture through a pressure vessel, then the syngas pressure was adjusted to the desired reaction pressure. After the indicated reaction time, the autoclave was cooled to room temperature and depressurized, then the reaction mixture was analyzed by GC with internal standard and correction factors.

*Variant B*: $[Rh(CO)_2acac]$ and the ligand were dissolved in toluene, and transferred into the autoclave. A pressure of 3 – 5 bar $CO/H_2$ (1:1) was applied, and the autoclave was heated within 30 min to the corresponding reaction temperature while the mixture was stirred (1000 $min^{-1}$). The autoclave was cooled to room temperature and depressurized. The olefin was added through a pressure vessel to the reaction mixture, which was then heated to the reaction temperature within 30 min. When this temperature was reached, the desired syngas pressure was applied. After the indicated reaction time, the autoclave was cooled to room temperature and depressurized, and the reaction mixture analyzed by GC with internal standard and correction factors.

**Hydroformylation of oct-2-ene**

*a) Rhodium/phosphinine catalyst*: Oct-2-ene (*Z*/*E* 80:20) (24.8 g, 221 mmol) in toluene (24.9 g) was completely converted by treating it with $[Rh(CO)_2acac]$ (7.9 mg, 0.03 mmol) and phosphinine **8** (0.2334 g, 0.61 mmol) at 90 °C and 10 bar $CO/H_2$ (1:1) for 4 h according to variant A. Product yields: 3-/4-octene (1 %), *n*-nonanal (24 %), 2-methyloctanal (43 %), 2-ethylhepatanal (18 %), and 2-propylhexanal (14 %). Aldehyde selectivity (99 %).

*b) Rhodium/triphenylphosphine catalyst*: Oct-2-ene in toluene (12.0 g, 108 mmol) was 69 % converted by treating it with $[Rh(CO)_2acac]$ (3.9 mg, 0.015 mmol) and triphenylphosphane (0.075 g, 0.29 mmol) at 90 °C and 10 bar $CO/H_2$ (1:1) for 4 h according to variant A. Product yields: 3-/4-octene (5 %), *n*-nonanal (3 %), 2-methyloctanal (42 %), 2-ethylhepatanal (17 %), and 2-propylhexanal (2 %). Aldehyde selectivity (95 %).

**Hydroformylation of isobutene**

*a) Rhodium/phosphinine catalyst*: Isobutene (15.7 g, 280 mmol) in toluene (15.0 g) was 85 % converted by treating it with $[Rh(CO)_2acac]$ (5 mg, 0.019 mmol) and phosphinine **8** (0.1326 g, 0.38 mmol) at 80 °C and 30 bar $CO/H_2$ (1:1) for 4 h according to variant B. Product yield: Isovaleraldehyde 85 %; aldehyde selectivity = 99 %; regioselectivity = 99 %.

*b) Rhodium/triphenylphosphine catalyst*: isobutene (15.7 g, 280 mmol) in toluene (15.0 g) was 9 % converted by treating it with $[Rh(CO)_2acac]$ (5 mg, 0.019 mmol) and triphenylphosphane (0.099 g, 0.38 mmol) at 80 °C and 30 bar $CO/H_2$ (1:1) for 4 h according to variant B. Product yield: isovaleraldehyde = 8 %.

**Hydroformylation of methallyl alcohol**

*a) Rhodium/phosphinine catalyst*: A methallyl alcohol conversion of 94 % was obtained by allowing $[Rh(CO)_2acac]$ (3.1 mg, 0.012 mmol), phosphinine **8** (0.091 g, 0.024 mmol), and isobutene (3.61 g, 50 mmol) in toluene (15.0 mL) to react at 90 °C and 20 bar $CO/H_2$ (1:1) for 120 min according to variant A. Product yield: 3-methyl-γ-lactol = 94 %; aldehyde selectivity = 99 %; regioselectivity = 99 %.

*b) Rhodium/triphenylphosphine catalyst*: a methallylic alcohol conversion of 88 % was obtained by reacting $[Rh(CO)_2acac]$ (3.1 mg, 0.012 mmol), triphenylphosphane (0.063 g, 0.024 mmol) and isobutene (3.61 g, 50 mmol) in toluene (15.0 mL) at 90 °C and 20 bar $CO/H_2$ (1:1) for 300 min according to variant A. Product yield: 3-methyl-γ-lactol = 88 %; aldehyde selectivity = 99 %; regioselectivity = 99 %).

**Hydroformylation of (−)-α-pinene**: an α-pinene conversion of 13 % was obtained from reacting $[Rh(CO)_2acac]$ (4.9 mg, 0.019 mmol), phosphinine **8** (0.144 g, 0.38 mmol) and (−)-α-pinene (17.9 g, 132 mmol) in toluene (22 mL) at 80 °C and 60 bar $CO/H_2$ (1:1) for 16 h according to variant A. Aldehyde selectivity = 99 %; regio- and diastereoselectivity = 90 %. The product was purified through distillation and subsequent flash chromatography on silica with petroleum ether/ethyl acetate (19:1) to furnish (−)-*endo*-3-formylpinane as a colorless oil; yield: 2.085 g, 9.5 %. Spectroscopic and analytical data correspond to those reported previously.[55]

**Hydroformylation of 2,3-dimethylbut-2-ene**

*a) Rhodium/phosphinine catalyst*: 2,3-dimethylbut-2-ene (25.3 g, 300.6 mmol) in toluene (25 g) was 29.2 % converted by treating it with $[Rh(CO)_2acac]$ (8 mg, 0.031 mmol) and phosphinine **8** (0.2628 g, 0.69 mmol) at 100 °C and 60 bar $CO/H_2$ (1:1) for 24 h according to variant A. Yield: 3,4-dimethylpentanal = 29.2 %; aldehyde selectivity = 99 %; regioselectivity = 99 %.

*b) Rhodium/triphenylphosphine catalyst*: 2,3-dimethylbut-2-ene (24.1 g, 286.4 mmol) in toluene (25 g) was 0.5 % converted by treating it with $[Rh(CO)_2acac]$ (7.2 mg, 0.028 mmol) and phosphinine **8** (161.8 mg, 0.617 mmol) at 100 °C and 60 bar $CO/H_2$ (1:1) for 24 h according to variant A. Yield: 3,4-dimethylpentanal = 0.5 %; aldehyde selectivity = 99 %; regioselectivity = 99 %).

**Hydroformylation of 3-methylbut-3-en-1-ol (isoprenol)**: isoprenol (6.2 g, 70 mmol) in toluene (6.0 g) was 73 % converted by treating it with $[Rh(CO)_2acac]$ (1.8 mg, 0.007 mmol) and phosphinine **8** (48.1 mg, 0.127 mmol) at 80 °C and 40 bar $CO/H_2$ (1:1) for 24 h according to variant A. Yield: 4-methyl-3,4,5,6-tetrahydro-2H-pyran-2-ol = 73 %; aldehyde selectivity = 99 %; regioselectivity = 99 %).

## Acknowledgments

This work was supported by the Fonds der Chemischen Industrie and the Alfried Krupp Award for young university teachers of the Krupp Foundation, as well as by BASF AG.

[1] K. Weissermel, H.-J. Arpe, *Industrielle Organische Chemie*, VCH, Weinheim, **1988**, pp. 133 – 148.
[2] B. Breit, W. Seiche, *Synthesis* **2001**, 1 – 36.
[3] D. Evans, J. A. Osborn, G. Wilkinson, *J. Chem. Soc. A* **1968**, 3133 – 3142.
[4] Recent reviews: a) J. A. Moulijn, P. W. N. M. van Leeuwen, R. A. van Santen, *Studies in Surface Science and Catalysis*, *Vol. 79*: *Catalysis—An Integrated Approach to Homogeneous, Heterogeneous and Industrial Catalysis*, Elsevier, Amsterdam, **1993**; b) C. D. Frohning, C. W. Kohlpaintner in *Applied Homogeneous Catalysis with Organometallic Compounds*, (Eds.: B. Cornils, W. A. Herrmann), VCH, Weinheim, **1996**, Chapter 2, pp. 29 – 104; c) M. Beller, B. Cornils, C. D. Frohning, C. W. Kohlpaintner, *J. Mol. Cat. A* **1995**, *104*, 17 – 85.
[5] C. P. Casey, G. T. Whiteker, *Isr. J. Chem.* **1990**, *30*, 299 – 304.
[6] B. Breit, *Chem. Eur. J.* **2000**, *6*, 1519 – 1524.
[7] a) S. D. Burke, J. E. Cobb, *Teterahedron Lett.* **1986**, *27*, 4237 – 4240; b) W. R. Jackson, P. Perlmutter, E. E. Tasdelen, *J. Chem. Soc. Chem. Commun.* **1990**, 763 – 764.
[8] a) B. Breit, *Angew. Chem.* **1996**, *108*, 3021 – 3023; *Angew. Chem. Int. Ed. Engl.* **1996**, *35*, 2835 – 2837; b) B. Breit, *Liebigs Ann.* **1997**, 1841 – 1851; B. Breit, M. Dauber, K. Harms, *Chem. Eur. J.* **1999**, *5*, 2819 – 2827; c) B. Breit, *J. Chem. Soc. Chem. Commun.* **1997**, 591 – 592; d) B.

  0947-6539/01/0714-3120 $ 17.50+.50/0 

Breit, *Eur. J. Org. Chem.* **1998**, 1123–1134; e) B. Breit, *Tetrahedron Lett.* **1998**, *39*, 5163–5166; f) B. Breit, S. K. Zahn, *Angew. Chem.* **1999**, *111*, 1022–1024; *Angew. Chem. Int. Ed.* **1999**, *38*, 969–971.

[9] a) K. Nozaki, I. Ojima in *Catalytic Asymmetric Synthesis* 2nd ed. (Ed.: I. Ojima), Wiley-VCH, New York, **2000**, Chapter 7, pp. 429–463; b) F. Agbossou, J.-F. Carpentier, A. Mortreux, *Chem. Rev.* **1995**, *95*, 2485–2506; c) S. Gladiali, J. C. Bayón, C. Claver, *Tetrahedron: Asymmetry* **1995**, *6*, 1453–1474.

[10] B. Heil, L. Markó, *Chem. Ber.* **1969**, *102*, 2238–2240.

[11] a) R. L. Pruett, J. A. Smith, *J. Org. Chem.* **1969**, *34*, 327–330; b) P. W. N. M. van Leeuwen, C. F. Roobeek, *J. Organomet. Chem.* **1983**, *258*, 343–350.

[12] T. Jongsma, G. Challa, P. W. N. M. van Leeuwen, *J. Organomet. Chem.* **1991**, *421*, 121–128.

[13] D. Selent, K.-D. Wiese, D. Röttger, A. Börner, *Angew. Chem.* **2000**, *112*, 1694–1696; *Angew. Chem. Int. Ed.* **2000**, *39*, 1639–1641.

[14] a) A. M. Trzeciak, J. J. Ziólkowski, *Coord. Chem. Rev.* **1999**, *190–192*, 883–900; b) L. A. van der Veen, P. C. J. Kamer, P. W. N. M. van Leeuwen, *Angew. Chem.* **1999**, *111*, 349–351; *Angew. Chem. Int. Ed.* **1999**, *38*, 336–338.

[15] a) G. Märkl in *Multiple Bonds and Low Coordination in Phosphorus Chemistry* (Eds.: M. Regitz, O. J. Scherer) Thieme, **1990**, pp. 220–257; b) F. Mathey, *Rev. Heteroat. Chem.* **1992**, 6, 1–24; c) G. Märkl, *Angew. Chem.* **1966**, *78*, 907–908; *Angew. Chem. Int. Ed. Engl.* **1966**, *5*, 846–847.

[16] For the use of $\eta^6$-phosphabenzene iron complexes as catalysts for pyridine formation see: F. Knoch, F. Kremer, U. Schmidt, U. Zenneck, P. Le Floch, F. Mathey, *Organometallics* **1996**, *15*, 2713–2719; see also ref. [19].

[17] a) C. Batich, E. Heilbronner, V. Hornung, A. J. Ashe III, D. T. Clark, U. T. Cobley, D. Kilcast, I. Scanlan, *J. Am. Chem. Soc.* **1973**, *95*, 928–930; b) A. J. Ashe III, F. Burger, M. Y. El-Sheik, E. Heilbronner, J. P. Maier, J.-F. Muller, *Helv. Chim. Acta* **1976**, *59*, 1944–1948.

[18] a) W. J. Hehre, R. Ditchfield, R. F. Stewart, J. A. Pople, *J. Chem. Phys.* **1970**, *52*, 2769–2773; b) G. Frison, A. Sevin, N. Avarvari, F. Mathey, P. Le Floch, *J. Org. Chem.* **1999**, *64*, 5524–5529.

[19] a) B. Breit, *J. Chem. Soc. Chem. Commun.* **1996**, 2071–2072; b) B. Breit, R. Winde, K. Harms, *J. Chem. Soc. Perkin Trans. 1* **1997**, 2681–2682; c) B. Breit, R. Paciello, B. Geissler, M. Röper (BASF AG) DE 19.621.967, **1997** (EP 906 261, WO 97/46 507); [*Chem. Abstr.* **1998**, *128*, 129.496]; R. Paciello, T. Mackewitz, M. Röper, B. Breit (BASF AG) DE 19.911.920, **2000** (WO 00/55 164); [*Chem. Abstr.* **2000**, *133*, 238.120.

[20] G. Märkl, F. Lieb, A. Merz, *Angew. Chem.* **1967**, *79*, 947–948; *Angew. Chem. Int. Ed. Engl.* **1967**, *6*, 944–945.

[21] R. Paciello, E. Zeller, B. Breit, M. Röper (BASF AG) DE 19.743.197, **1999** (EP 1 025 111, WO 99/16774); [*Chem. Abstr.* **1999**, *130*, 237 700u]; T. Mackewitz, M. Röper (BASF AG) DE 19.911.922, **2000** (EP 1036 796); [*Chem. Abstr.* **2000**, *133*, 239 110].

[22] K. Dimroth, C. Reichardt, K. Vogel, *Org. Synth. Coll. Vol. V*, 1135–1137.

[23] A. Garcia-Raso, J. Garcia-Raso, B. Campaner, R. Mestres, J. V. Sinisterra, *Synthesis* **1982**, 1037–1041.

[24] P. F. G. Praill, A. L. Whitear, *J. Chem. Soc.* **1961**, 3573–3579.

[25] W. Rösch, M. Regitz, *Z. Naturforsch.* **1986**, *41b*, 931–933.

[26] S. Voß, Ph.D. thesis, Universität Marburg (Germany), **1998**.

[27] S. Berger, S. Braun, H.-O. Kalinowski, *NMR-Spektroskopie von Nichtmetallen*, *Vol. 3*, Thieme, Stuttgart, **1993**, pp. 164–166.

[28] Compare $[Rh_4(CO)_{12}]$, $^{13}C$ NMR ($CH_2Cl_2$): $\delta = 190.3$; see: H.-O. Kalinowski, S. Berger, S. Braun, *$^{13}C$-NMR-Spektroskopie*, Thieme, Stuttgart, **1984**, p. 383.

[29] Compare $[Rh(CO)_2acac]$: For the CO ligand $^1J(C,Rh) = 73$ Hz; see ref. [28] p. 550; for another example see ref. [8d].

[30] K. G. Moloy, J. L. Petersen, *J. Am. Chem. Soc.* **1995**, *117*, 7696–7710.

[31] E. Fernández, A. Ruiz, C. Claver, S. Castillón, A. Polo, J. F. Piniella, A. Alvarez-Larena, *Organometallics* **1998**, *17*, 2857–2864.

[32] a) M. Li Wu, M. J. Desmond, R. S. Drago, *Inorg. Chem.* **1979**, *18*, 679–686; b) K. R. Dunbar, S. C. Haefner, *Inorg. Chem.* **1992**, *31*, 3676–3679; c) A. Ceriotti, G. Ciani, A. Sironi, *J. Organomet. Chem.* **1983**, *247*, 345–350; d) P. A. Chaloner, C. Claver, P. B. Hitchcock, A. M. Masdue, A. Ruiz, *Acta Crystallogr.* **1991**, *C47*, 1307–1308.

[33] C. A. Tolman, *Chem. Rev.* **1977**, *77*, 313–348.

[34] From PM3 calculations for complex **26** (M = Rh) with the PCSpartan software package.

[35] a) Y. Ohgomori, S. Yoshida, Y. Watanabe, *J. Chem. Soc. Dalton Trans.* **1987**, 2969–2974; b) D. de Montauzon, R. Poilblanc, *J. Organomet. Chem.* **1975**, *93*, 397–404; c) T. Sakakura, T. Sodeyama, K. Sasaki, K. Wada, M. Tanaka, *J. Am. Chem. Soc.* **1990**, *112*, 7221–7229.

[36] a) D. Evans, J. A. Osborn, G. Wilkinson, *Inorg. Synth.* **1990**, *28*, 79–80; b) S. Franks, F. R. Hartley, *Inorg. Chim. Acta* **1981**, *47*, 235–248; c) G. M. Intille, *Inorg. Chem.* **1972**, *11*, 695–702; d) A. J. Deeming, B. L. Shaw, *J. Chem. Soc. A* **1969**, 597–602; e) J. A. McCleverty, G. Wilkinson, *Inorg. Synth.* **1966**, *8*, 214–217.

[37] R. P. Hughes in *Comprehensive Organometallic Chemistry* (Eds.: G. Wilkinson, F. G. A. Stone, E. W. Abel), Pergamon, Oxford, **1982**, Chapter 35, pp. 296ff.

[38] J. M. Brown, A. G. Kent, *J. Chem. Soc. Perkin Trans. 2* **1987**, 1597–1607.

[39] M. Kranenburg, Y. E. M. van der Burgt, P. C. J. Kamer, P. W. N. M. van Leeuwen, *Organometallics* **1995**, *14*, 3081–3089.

[40] D. T. Brown, T. Eguchi, B. T. Heaton, J. A. Iggo, R. Whyman, *J. Chem. Soc. Dalton Trans.* **1991**, 677–683.

[41] Tested for ligands **3** and **8**.

[42] A. van Rooy, E. N. Orij, P. C. J. Kamer, P. W. N. M. van Leeuwen, *Organometallics* **1995**, *14*, 34–43.

[43] W. F. Gresham, R. E. Brooks, (DuPont de Nemours & Co.) US 2.497.303, **1950**; [*Chem. Abstr.* **1950**, *44*, 4492e].

[44] *Organikum*, 19th ed., Deutscher Verlag der Wissenschaften, Leipzig, **1993**, p. 469.

[45] G. Becker, H. Schmidt, G. Uhl, W. Uhl, M. Regitz, W. Rösch, U.-J. Vogelbacher, *Inorg. Synth.* **1990**, *27*, 243–253.

[46] R. E. Lutz, T. A. Martin, J. F. Codington, T. M. Amacker, R. K. Allison, N. H. Leake, R. J. Rowlett, J. D. Smith, J. W. Wilson III, *J. Org. Chem.* **1949**, *14*, 982–1000.

[47] C. Reichardt, R. Müller, *Liebigs Ann. Chem.* **1976**, 1937–1952.

[48] N. A. Portnoy, C. J. Morrow, M. S. Chattha, J. C. Williams, A. M. Aguiar, *Tetrahedron Lett.* **1971**, 1401–1402.

[49] J. A. Durden, D. G. Crosby, *J. Org. Chem.* **1965**, *30*, 1684–1687.

[50] F. Lieb, Ph.D. thesis, Universität Würzburg (Germany), **1970**.

[51] G. Märkl, F. Lieb, A. Merz, *Angew. Chem.* **1967**, *79*, 475; *Angew. Chem. Int. Ed. Engl.* **1967**, *6*, 458–459.

[52] A. R. Katritzky, J. Arrowsmith, Z. bin Bahari, C. Jayaram, T. Siddiqui, S. Vassilatos, *J. Chem. Soc. Perkin Trans. 1* **1980**, 2851–2855.

[53] G. M. Sheldrick, SHELXS-96, Program for solving crystal structures, University of Göttingen, **1997**.

[54] G. M. Sheldrick, SHELXL-97, Program for refining crystal structures, University of Göttingen, **1997**.

[55] F. Langer, K. Püntener, R. Stürmer, P. Knochel, *Tetrahedron: Asymmetry* **1997**, *8*, 715–738.

Received: January 22, 2001 [F3017]